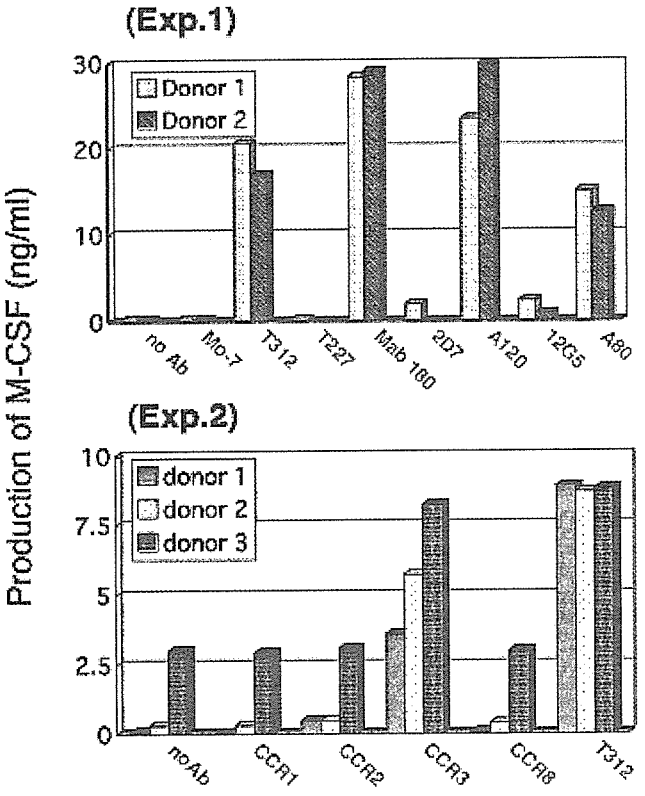

Figure 9. Screening of the other anti-chemokine receptor mAbs that can stimulate monocytes. Purified monocytes at 1×10^5/ml in RPMI medium were cultured in wells precoated with various mAbs overnight, and the culture supernatants were assayed for M-CSF by ELISA. The values depicted represent the mean of triplicate cultures with SD of <10%.

effective as T312 mAb in the stimulation of monocytes. Among the anti-human CXCR4 mAbs, clone A120 (rat IgG2b anti-CXCR4 ECL1&2) and A80 (rat IgG1 anti-CXCR4 ECL-3) were also capable of stimulating monocytes. Another monocyte-stimulating mAb was the rat IgG2a anti-CCR3 mAb. These mAbs that successfully stimulated monocytes also promoted monocyte adhesion, and A120 anti-CXCR4 mAb in particular was very potent in inducing adhesion and differentiation of monocytes similar to the data derived using the T312 mAb (data not shown). Whether subtle differences exist in the adherent cells enriched by the mAbs that were active in such an assay remains to be determined.

Discussion

In the present study, we present data showing that cross-linking of CCR5 as well as select other chemokine receptors (CXCR4 and CCR3) by mAbs immobilized onto plastic microtiter wells leads to enhanced adhesion of monocytes followed by synthesis of M-CSF and a set of β-chemokines and that incubation of these adherent cells with GM-CSF and IL-4 or IL-4 alone leads to their differentiation along the DC lineage. This functional activity observed following chemokine receptor cross-linking is in contrast to the data obtained with FcR cross-linking (34). This enhanced adherence of monocytes apparently improves the efficacy of adhesion-based monocyte enrichment from fresh PBMCs.

One contributing mechanism that facilitates such tight adhesion may involve the enhanced affinity of the β2-integrins Mac-1 and/or p150/95, which bind to fibrinogen, an extracellular matrix protein, since such adhesion was markedly inhibited in the presence of mAb anti-CD18 (a common chain of the β2-integrin) but not anti-CD11a (a component of another β2-integrin, LFA-1). This view is supported by data obtained by flow cytometric analysis of the T312 mAb-stimulated monocytes, compared to those incubated in control mAb-coated wells. Thus, the T312 mAb-stimulated cells but not the control cells showed a markedly increased density of staining with FITC-fibrinogen, but not with FITC-gelatin or collagen (data not shown). Although sensitization of chemokine receptors by their respective cognate chemokine ligands is known to activate β1- and β2-integrins (5), it is important to note that the addition or precoating of wells with chemokines that bind to CCR5 (i.e., RANTES, MIP-1α, and MIP-1β), respectively, did not induce such enhanced monocyte adhesion *in vitro* in the present study (data not shown). Thus, it is likely that antibody-mediated cross-linking of chemokine receptors initiates an enhanced degree of activation of monocytes, probably through an extraordinary degree of polarization of the receptors onto the plates. This is supported by the observations made by Lee *et al.* (35) that the mode of monocyte activation by cross-linking of chemokine receptors by gp120 of HIV-1 particles was stronger than that induced by a simple interaction between CCR5 and CXCR4 with their respective chemokines. The inhibition of the T312 mAb-induced monocyte adhesion by the PI3-K-specific inhibitor LY294.002 indicates that the T312 mAb-mediated CCR5 cross-linking also stimulates the G-protein signal cascade, as documented previously for gp120 of HIV-1 (35) and chemokines (36). Since PI3-K activation by chemokines also induces polarization of adhesion molecules and facilitates migration (5, 37), it is likely that it is either the mere strength of the signal that is induced by cross-linking of CCR5 by T312 mAb or the potential pulling together of additional, as-yet-unknown proteins that distinguishes between enhanced adhesion and mere signaling.

It is worth noting that the tight adhesion was not induced by another rat IgG anti-CCR5 mAb, termed clone T227. The difference between anti-CCR5 clone T312 and T227 is that the T227 mAb recognizes a region located within the N-terminus of the CCR5 molecule that has been further localized to a peptide spanning the CCR5 N-terminus amino acids 1–20 but not 2–21, whereas the clone T312 mAb recognizes both of the peptides, with an affinity similar to the clone T227 mAb (Tanaka *et al.*, unpublished data). These two mAbs compete with each other in binding to CCR5. Thus, these results indicate that activation of monocyte by CCR5 cross-linking is epitope-dependent

rather than antibody affinity-dependent. This view is further supported by the observation that the use of yet another immobilized CCR5-specific clone, ECL-2 mAb, did not lead to enhanced adhesion of monocytes, indicating a requirement for epitope specificity to facilitate adhesion. Similarly, with regard to CXCR4, the clones A145 mAb (anti–N-terminus) and 12G5 (anti-ECL1&2) did not induce significant monocyte adhesion, in contrast to A120 mAb (anti-ECL1&2) and A80 mAb (anti–ECL-3). The clone A120 mAb blocks the binding of SDF-1 (the natural ligand for CXCR4) and inhibits infection by the CXCR4-tropic HIV-1 strains, whereas the clone A80 mAb does not block SDF-1 binding but stimulates homologous T-cell aggregation and thus enhances infection of the CXCR4 and CCR5-tropic HIV-1 strains (25). However, it is still unclear which regions (epitopes) of each chemokine receptor are the hot spots for the induction of strong activation signals on monocytes, and this topic thus requires further study.

Along with the enhanced adhesion facilitated by cross-linking of the chemokine receptor, such cross-linking also induced downmodulation of cell surface expression of CD14, CD4, CCR5, and CXCR4 and cytokine production by monocytes. It is of interest that similar effects on monocytes have been induced by prokineticin 1 (PK1)/endocrine gland-derived vascular endothelial growth factor (EG-VEGF), and its G protein-coupled receptors (PKR1 and PKR2) (38). Downregulation of CD14 was reported to be induced by IL-4 or IL-13 at the transcriptional level (39) or by shedding, which was induced by antibody-mediated cross-linking of CD14 or stimulation by LPS and IFN-γ (40). However, these are not the likely mechanisms in studies reported herein, since there was little if any production of IL-4 and IL-13 and no detectable levels of soluble CD14 in the culture supernatants. It has been shown that downmodulation of cell surface expression of CD14, CD4, and CXCR4, but not CCR5 on monocytes, is induced by PKC activation by phorbol 12-myristate 13-acetate (PMA) (41, 42) and that CCR5 downmodulation is induced by CCR5-binding chemokines at only high concentrations as a result of CCR5 internalization (43). Whether these pathways are activated by cross-linking of the chemokine receptors is currently not known. It has also been shown that there is a molecular association between CD4 and the chemokine receptors or among the various chemokine receptors (44, 45). Thus, it can be speculated that CCR5 or CXCR4 cross-linking may induce homo- or hetero-oligomerization of the cell surface CD14, CD4, CXCR4, and/or CCR5, and is then internalized.

In the early studies on monocyte adhesion (5) it was shown that adherence onto plastic plates stimulates monocytes to activate M-CSF, IL-1β, or TNF-α gene expression and that LPS stimulation further enhances the synthesis of these cytokines. Similarly, activation of monocytes via the PK1 pathway following adhesion requires additional stimulation by LPS to promote the production of IL-12 p70 and TNF-α (46). Thus, it is clear that the mechanisms for cytokine production in the studies described herein likely involve distinct pathways other than those discussed above. In addition, the addition of soluble chemokines or the use of immobilized chemokines with specificity for CCR5 and CXCR4 did not induce cytokine production in the present conditions (data not shown). Differences in the precise pathways that are triggered in the studies reported herein are a subject of current study.

The observation that not only CCR5 but also CXCR4 and CCR3 cross-linking triggered production of M-CSF by monocytes and induced differentiation in the absence of exogenously added M-CSF or GM-CSF was unexpected. For differentiation of monocytes into macrophages *in vitro* in the absence of these cytokines, extracellular matrix proteins are known to have profound influence (47). It has been previously reported that human monocytes differentiated into CD14-low macrophages in a fibronectin-containing medium without the addition of exogenous cytokines (48). Thus, bovine fibronectin in our RPMI medium may have some additive effects on chemokine receptor–stimulated monocyte differentiation, although the use of serum-free medium for monocyte cultivation in T312 mAb-coated wells did not influence the present results (data not shown). Although cross-linking of CCR5, CXCR4, or CCR3 resulted in M-CSF production from monocytes, anti-M-CSF– or GM-CSF–neutralizing mAbs did not block monocyte differentiation into macrophages (data not shown). Thus, we assume that chemokine receptor cross-linking may bypass the requirement of M-CSF stimulation. Since the ligation of M-CSF receptor (CD115) stimulates PI3-K (49, 50), the PI3-K activation as a result of the chemokine receptor cross-linking may be responsible for the *de novo* monocyte differentiation into macrophages. The mechanisms by which cross-linking of chemokine receptors on monocytes induced the differentiation of these cells into DCs without the addition of exogenous GM-CSF in the presence of IL-4 are also under current study. The cross-linking may function as survival and differentiation factor for the generation of DCs from monocytes, because monocytes in the absence of chemokine receptor cross-linking failed to survive when cultured in media containing IL-4 alone.

The primary objective of the present study was to find an alternate, more-efficient and practical method for the *in vitro* generation of functional DCs with potent Th1-inducing capacity *in vivo*. Various cytokine cocktails have been applied for generation of functional DCs, including combinations of IL-3 and IFN-β, Flt3L and IL-4, CD40L alone, or GM-CSF, IL-4, and the proinflammatory cytokines GM-CSF and Type I IFN (51–56). In addition, it has been reported that the methods of monocyte isolation, such as adherence or $CD14^+$ enrichment by MACS (which results in CD14 cross-linking), influence cytokine production from generated DCs (i.e., adherent monocyte-derived DCs were more potent in producing IL-12, IL-10, and TNF-α and in stimulating Tc1 than those from CD14 positively selected

monocytes) (24). Because the DCs generated in the studies reported herein by CCR5 (or CXCR4 or CCR3) cross-linking in the presence of either GM-CSF and IL-4 or IL-4 alone were relatively more potent than conventional DCs in stimulating IFN-γ production from allogeneic naïve $CD4^+$ T cells *in vitro* and OVA- or KLH-specific T cells *in vivo*, it is indicated that in studies that require Th1-polarizing DCs, the cross-linking of CCR5, CXCR4, or CCR3 on monocytes should be considered. The higher density of expression of CD86 on the chemokine receptor cross-linked DCs may have some influence for Th1-inducing capacity, although the mechanism at present still remains unknown.

Based on the results of the present study, we suggest that the use of cross-linking of CCR5, CXCR4, or other chemokine receptors for the generation of functional DCs *ex vivo* provides an alternate and simple tool that will facilitate the therapeutic use of DCs. Thus, studies of DC-based immunotherapy in patients with HIV-1 infection that have been reasoned to require induction of maintenance of Th1 type of antiviral immune response could benefit from such an approach. In addition, cross-linking of the chemokine receptors could also facilitate limited entry of HIV-1 into such cells because of downmodulation of the HIV-1 receptors. Such an approach has already been initiated, and preliminary studies have shown that inactivated HIV-1–pulsed DCs generated from CCR5– and CXCR4–cross-linked monocytes could trigger highly potent human anti–HIV-1 T-cell responses using our hu-PBL-SCID mouse model. These studies are currently in progress.

We thank the NIH AIDS Research and Reference Reagent Program for supplying IL-2.

1. van Furth R, Cohn ZA. The origin and kinetics of mononuclear phagocytes. J Exp Med 128:415–435, 1968.
2. Warren MK, Vogel SN. Bone marrow-derived macrophages: development and regulation of differentiation markers by colony-stimulating factor and interferons. J Immunol 134:982–989, 1985.
3. Steinman RM. The dendritic cell system and its role in immunogenicity. Annu Rev Immunol 9:271–296, 1991.
4. Zhou LJ, Tedder TF. CD14+ blood monocytes can differentiate into functionally mature CD83+ dendritic cells. Proc Natl Acad Sci U S A 93:2588–2592, 1996.
5. Imhof BA, Aurrand-Lions M. Adhesion mechanisms regulating the migration of monocytes. Nat Rev Immunol 4:432–444, 2004.
6. Mellado M, Rodriguez-Frade JM, Manes S, Martinez AC. Chemokine signaling and functional responses: the role of receptor dimerization and TK pathway activation. Annu Rev Immunol 19:397–421, 2001.
7. Pulendran B, Palucka K, Banchereau J. Sensing pathogens and tuning immune responses. Science 293:253–256, 2001.
8. Donaghy H, Pozniak A, Gazzard B, Qazi N, Gilmour J, Gotch F, Patterson S. Loss of blood CD11c(+) myeloid and CD11c(–) plasmacytoid dendritic cells in patients with HIV-1 infection correlates with HIV-1 RNA virus load. Blood 98:2574–2576, 2001.
9. Soumelis V, Scott I, Gheyas F, Bouhour D, Cozon G, Cotte L, Huang L, Levy JA, Liu YJ. Depletion of circulating natural type 1 interferon-producing cells in HIV-infected AIDS patients. Blood 98:906–912, 2001.
10. Urban BC, Ferguson DJ, Pain A, Willcox N, Plebanski M, Austyn JM, Roberts DJ. Plasmodium falciparum-infected erythrocytes modulate the maturation of dendritic cells. Nature 400:73–77, 1999.
11. Fugier-Vivier I, Servet-Delprat C, Rivailler P, Rissoan MC, Liu YJ, Rabourdin-Combe C. Measles virus suppresses cell-mediated immunity by interfering with the survival and functions of dendritic and T cells. J Exp Med 186:813–823, 1997.
12. Fong L, Engleman EG. Dendritic cells in cancer immunotherapy. Annu Rev Immunol 18:245–273, 2000.
13. Lu W, Arraes LC, Ferreira WT, Andrieu JM. Therapeutic dendritic-cell vaccine for chronic HIV-1 infection. Nat Med 10:1359–1365, 2004.
14. Garcia F, Lejeune M, Climent N, Gil C, Alcami J, Morente V, Alos L, Ruiz A, Setoain J, Fumero E, Castro P, Lopez A, Cruceta A, Piera C, Florence E, Pereira A, Libois A, Gonzalez N, Guila M, Caballero M, Lomena F, Joseph J, Miro JM, Pumarola T, Plana M, Gatell JM, Gallart T. Therapeutic immunization with dendritic cells loaded with heat-inactivated autologous HIV-1 in patients with chronic HIV-1 infection. J Infect Dis 191:1680–1685, 2005.
15. Lu W, Wu X, Lu Y, Guo W, Andrieu JM. Therapeutic dendritic-cell vaccine for simian AIDS. Nat Med 9:27–32, 2003.
16. Yosida A, Tanaka R, Murakami T, Takahashi Y, Koyanagi Y, Nakamura M, Ito M, Yamamoto N, Tanaka Y. Induction of protective immune responses against R5 human immunodeficiency virus type 1 (HIV-1) infection in hu-PBL-SCID mice by intrasplenic immunization with HIV-1–pulsed dendritic cells: possible involvement of a novel factor of human $CD4^+$ T-cell origin. J Virol 77:8719–8728, 2003.
17. Lapenta C, Santini SM, Logozzi M, Spada M, Andreotti M, Di Pucchio T, Parlato S, Belardelli F. Potent immune response against HIV-1 and protection from virus challenge in hu-PBL-SCID mice immunized with inactivated virus-pulsed dendritic cells generated in the presence of IFN-alpha. J Exp Med 198:361–367, 2003.
18. Wu L, Dakic A. Development of dendritic cell system. Cell Mol Immunol 1:112–118, 2004.
19. Banchereau J, Steinman RM. Dendritic cells and the control of immunity. Nature 392:245–252, 1998.
20. D'Amico A, Wu L. The early progenitors of mouse dendritic cells and plasmacytoid predendritic cells are within the bone marrow hemopoietic precursors expressing Flt3. J Exp Med 198:293–303, 2003.
21. Romani N, Reider D, Heuer M, Ebner S, Kampgen E, Eibl B, Niederwieser D, Schuler G. Generation of mature dendritic cells from human blood. An improved method with special regard to clinical applicability. J Immunol Methods 196:137–151, 1996.
22. Sallusto F, Lanzavecchia A. Efficient presentation of soluble antigen by cultured human dendritic cells is maintained by granulocyte/macrophage colony-stimulating factor plus interleukin 4 and downregulated by tumor necrosis factor alpha. J Exp Med 179:1109–1118, 1994.
23. Tuyaerts S, Noppe SM, Corthals J, Breckpot K, Heirman C, De Greef C, Van Riet I, Thielemans K. Generation of large numbers of dendritic cells in a closed system using Cell Factories. J Immunol Methods 264: 135–151, 2002.
24. Elkord E, Williams PE, Kynaston H, Rowbottom AW. Human monocyte isolation methods influence cytokine production from in vitro generated dendritic cells. Immunology 114:204–212, 2005.
25. Tanaka R, Yoshida A, Murakami T, Baba E, Lichtenfeld J, Omori T, Kimura T, Tsurutani N, Fujii N, Wang ZX, Peiper SC, Yamamoto N, Tanaka Y. Unique monoclonal antibody recognizing the third extracellular loop of CXCR4 induces lymphocyte agglutination and enhances human immunodeficiency virus type 1-mediated syncytium formation and productive infection. J Virol 75:11534–11543, 2001.
26. Grage-Griebenow E, Flad HD, Ernst M. Heterogeneity of human peripheral blood monocyte subsets. J Leukoc Biol 69:11–20, 2001.
27. Ohteki T, Fukao T, Suzue K, Maki C, Ito M, Nakamura M, Koyasu S. Interleukin 12-dependent interferon gamma production by CD8alpha+ lymphoid dendritic cells. J Exp Med 189:1981–1986, 1999.
28. Tanaka Y, Zeng L, Shiraki H, Shida H, Tozawa H. Identification of a

neutralization epitope on the envelope gp46 antigen of human T cell leukemia virus type I and induction of neutralizing antibody by peptide immunization. J Immunol 147:354–360, 1991.

29. Inudoh M, Kato N, Tanaka Y. New monoclonal antibodies against a recombinant second envelope protein of hepatitis C virus. Microbiol Immunol 42:875–877, 1998.
30. Tozawa H, Andoh S, Takayama Y, Tanaka Y, Lee B, Nakamura H, Hayami M, Hinuma Y. Species-dependent antigenicity of the 34-kDa glycoprotein found on the membrane of various primate lymphocytes transformed by human T-cell leukemia virus type-I (HTLV-I) and simian T-cell leukemia virus (STLV-I). Int J Cancer 41:231–238, 1988.
31. Magaud JP, Sargent I, Mason DY. Detection of human white cell proliferative responses by immunoenzymatic measurement of bromodeoxyuridine uptake. J Immunol Methods 106:95–100, 1988.
32. Patarroyo M, Prieto J, Beatty PG, Clark EA, Gahmberg CG. Adhesion-mediating molecules of human monocytes. Cell Immunol 113:278–289, 1988.
33. Davis GE. The Mac-1 and p150,95 beta 2 integrins bind denatured proteins to mediate leukocyte cell-substrate adhesion. Exp Cell Res 200:242–252, 1992.
34. MacIntyre EA, Roberts PJ, Jones M, Van der Schoot CE, Favalaro EJ, Tidman N, Linch DC. Activation of human monocytes occurs on cross-linking monocytic antigens to an Fc receptor. J Immunol 142:2377–2383, 1989.
35. Lee C, Liu QH, Tomkowicz B, Yi Y, Freedman BD, Collman RG. Macrophage activation through CCR5- and CXCR4-mediated gp120-elicited signaling pathways. J Leukoc Biol 74:676–682, 2003.
36. Mellado M, Rodriguez-Frade JM, Manes S, Martinez AC. Chemokine signaling and functional responses: the role of receptor dimerization and TK pathway activation. Annu Rev Immunol 19:397–421, 2001.
37. Vicente-Manzanares M, Rey M, Jones DR, Sancho D, Mellado M, Rodriguez-Frade JM, del Pozo MA, Yanez-Mo M, de Ana AM, Martinez AC, Merida I, Sanchez-Madrid F. Involvement of phosphatidylinositol 3-kinase in stromal cell-derived factor-1 alpha-induced lymphocyte polarization and chemotaxis. J Immunol 163:4001–4012, 1999.
38. Dorsch M, Qiu Y, Soler D, Frank N, Duong T, Goodearl A, O'Neil S, Lora J, Fraser CC. PK1/EG-VEGF induces monocyte differentiation and activation. J Leukoc Biol 78:426–434, 2005.
39. Lauener RP, Goyert SM, Geha RS, Vercelli D. Interleukin 4 down-regulates the expression of CD14 in normal human monocytes. Eur J Immunol 20:2375–2381, 1990.
40. Bazil V, Strominger JL. Shedding as a mechanism of down-modulation of CD14 on stimulated human monocytes. J Immunol 147:1567–1574, 1991.
41. Signoret N, Oldridge J, Pelchen-Matthews A, Klasse PJ, Tran T, Brass LF, Rosenkilde MM, Schwartz TW, Holmes W, Dallas W, Luther MA, Wells TN, Hoxie JA, Marsh M. Phorbol esters and SDF-1 induce rapid endocytosis and down modulation of the chemokine receptor CXCR4. J Cell Biol 139:651–664, 1997.
42. Signoret N, Rosenkilde MM, Klasse PJ, Schwartz TW, Malim MH, Hoxie JA, Marsh M. Differential regulation of CXCR4 and CCR5 endocytosis. J Cell Sci 111:2819–2830, 1998.
43. Xiao X, Wu L, Stantchev TS, Feng YR, Ugolini S, Chen H, Shen Z, Riley JL, Broder CC, Sattentau QJ, Dimitrov DS. Constitutive cell surface association between CD4 and CCR5. Proc Natl Acad Sci U S A 96:7496–7501, 1999.
44. Rodriguez-Frade JM, del Real G, Serrano A, Hernanz-Falcon P, Soriano SF, Vila-Coro AJ, de Ana AM, Lucas P, Prieto I, Martinez-A C, Mellado M. Blocking HIV-1 infection via CCR5 and CXCR4 receptors by acting in trans on the CCR2 chemokine receptor. EMBO J 23:66–76, 2004.
45. Ugolini S, Moulard M, Mondor I, Barois N, Demandolx D, Hoxie J, Brelot A, Alizon M, Davoust J, Sattentau QJ. HIV-1 gp120 induces an association between CD4 and the chemokine receptor CXCR4. J Immunol 159:3000–3008, 1997.
46. Cosentino G, Soprana E, Thienes CP, Siccardi AG, Viale G, Vercelli D. IL-13 down-regulates CD14 expression and TNF-alpha secretion in normal human monocytes. J Immunol 155:3145–3151, 1995.
47. Juliano RL, Haskill S. Signal transduction from the extracellular matrix. J Cell Biol 120:577–585, 1993.
48. Jacob SS, Shastry P, Sudhakaran PR. Monocyte-macrophage differentiation in vitro: modulation by extracellular matrix protein substratum. Mol Cell Biochem 233:9–17, 2002.
49. Hamilton JA. CSF-1 signal transduction. J Leukoc Biol 62:145–155, 1997.
50. Varticovski L, Druker B, Morrison D, Cantley L, Roberts T. The colony stimulating factor-1 receptor associates with and activates phosphatidylinositol-3 kinase. Nature 342:699–702, 1989.
51. Carbonneil C, Aouba A, Burgard M, Cardinaud S, Rouzioux C, Langlade-Demoyen P, Weiss L. Dendritic cells generated in the presence of granulocyte-macrophage colony-stimulating factor and IFN-alpha are potent inducers of HIV-specific CD8 T cells. AIDS 17: 1731–1740, 2003.
52. Mohty M, Vialle-Castellano A, Nunes JA, Isnardon D, Olive D, Gaugler B. IFN-alpha skews monocyte differentiation into Toll-like receptor 7-expressing dendritic cells with potent functional activities. J Immunol 171:3385–3393, 2003.
53. Nagai T, Devergne O, Mueller TF, Perkins DL, van Seventer JM, van Seventer GA. Timing of IFN-beta exposure during human dendritic cell maturation and naive Th cell stimulation has contrasting effects on Th1 subset generation: a role for IFN-beta-mediated regulation of IL-12 family cytokines and IL-18 in naive Th cell differentiation. J Immunol 171:5233–5243, 2003.
54. Dauer M, Obermaier B, Herten J, Haerle C, Pohl K, Rothenfusser S, Schnurr M, Endres S, Eigler A. Mature dendritic cells derived from human monocytes within 48 hours: a novel strategy for dendritic cell differentiation from blood precursors. J Immunol 170:4069–4076, 2003.
55. Brossart P, Grunebach F, Stuhler G, Reichardt VL, Mohle R, Kanz L, Brugger W. Generation of functional human dendritic cells from adherent peripheral blood monocytes by CD40 ligation in the absence of granulocyte-macrophage colony-stimulating factor. Blood 92:4238–4247, 1998.
56. Buelens C, Bartholome EJ, Amraoui Z, Boutriaux M, Salmon I, Thielemans K, Willems F, Goldman M. Interleukin-3 and interferon beta cooperate to induce differentiation of monocytes into dendritic cells with potent helper T-cell stimulatory properties. Blood 99:993–998, 2002.

Potential role of natural killer cells in controlling growth and infiltration of AIDS-associated primary effusion lymphoma cells

Md. Zahidunnabi Dewan,[1,2] Hiroshi Terunuma,[3,4] Masakazu Toi,[5] Yuetsu Tanaka,[6] Harutaka Katano,[7] Xuewen Deng,[3] Hiroyuki Abe,[4] Tadashi Nakasone,[2] Naoki Mori,[8] Tetsutaro Sata[7] and Naoki Yamamoto[1,2,9]

[1]Department of Molecular Virology, Graduate School, Tokyo Medical and Dental University, 1-5-45 Yushima, Bunkyo-ku, Tokyo 113-8519; [2]AIDS Research Center, National institute of Infectious Disease, 1-23-1 Toyama, Shinjuku-ku, Tokyo 162-8640; [3]Biotherapy Institute of Japan, 2-4-8 Edagawa, Koutou-ku, Tokyo 135-0051; [4]Kudan Clinic, 1-9-5 Kudankita, Chiyoda-ku, Tokyo 102-0073; [5]Division of Clinical Trials and Research, Breast Cancer Research and Treatment Program, Tokyo Metropolitan Komagome Hospital, Tokyo Medical Center for Cancer and Infectious Disease, 3-18-22 Honkomagome, Bunkyo-ku, Tokyo 113-8677; [6]Department of Immunology, Faculty of Medicine, University of the Ryukyus, 207 Uehara, Nishihara, Okinawa 903-0215; [7]Department of Pathology, National Institute of Infectious Diseases, 1-23-1 Toyama, Shinjyuku-ku, Tokyo 162-8640; [8]Division of Molecular Virology and Oncology, Graduate School of Medicine, University of the Ryukyus, 207 Uehara, Nishihara, Okinawa 903-0215, Japan

(Received June 20, 2006/Revised August 3, 2006/Accepted August 4, 2006/Online publication September 25, 2006)

Natural killer (NK) cells are an important component of the innate immune response against microbial infections and tumors. Direct involvement of NK cells in tumor growth and infiltration has not yet been demonstrated clearly. Primary effusion lymphoma (PEL) cells were able to produce tumors and ascites very efficiently with infiltration of cells in various organs of T-, B- and NK-cell knock-out NOD/SCID/γc^{null} (NOG) mice within 3 weeks. In contrast, PEL cells formed small tumors at inoculated sites in T- and B-cell knock-out NOD/SCID mice with NK-cells while completely failing to infiltrate into various organs. Immunosupression of NOD/SCID by treatment with an antimurine TM-β1 antibody, which transiently abrogates NK cell activity *in vivo*, resulted in enhanced tumorigenicity and organ infiltration in comparison with non-treated NOD/SCID mice. Activated human NK cells inhibited tumor growth and infiltration in NOG mice. Our results suggest that NK cells play an important role in growth and infiltration of PEL cells, and activated NK cells could be a promising immunotherapeutic tool against tumor or virus-infected cells either alone or in combination with conventional therapy. The rapid and efficient engraftment of PEL cells in NOG mice also suggests that this new animal model could provide a unique opportunity to understand and investigate the mechanism of pathogenesis and malignant cell growth. (*Cancer Sci* 2006; 97: 1381–1387)

Primary effusion lymphoma (PEL) was originally identified in AIDS-associated immunodeficient patients and has been recognized by the World Health Organization as a distinct AIDS-related form of B-cell lymphoproliferative disorder.[1–3] PEL is a non-Hodgkin's type lymphoma derived from postgerminal center B cells.[4] The tumor clone is characteristically infected by the Kaposi's sarcoma-associated herpesvirus, formerly called human herpesvirus type 8 (HHV-8),[5] and most cases are coinfected with Epstein–Barr virus.[6,7] PEL shows a peculiar presentation involving lymphomatous effusions of serous cavities and only occasionally presents with a definable mass.[5]

Immunodeficient mouse models of human malignancy have contributed significantly to understanding the pathogenesis of diseases as well as therapeutic purpose. The congenitally athymic and hairless nude mouse lacking functional T cells has been utilized as a host for human xenotransplantations for 30 years.[8] Thereafter, severe combined immunodeficiency (SCID) mice were found to have a genetic defect preventing functional development of T and B lymphocytes,[9,10] and can be engrafted successfully with a variety of normal hematopoietic and neoplastic cells.[11,12] In comparison with conventional SCID, the NOD-SCID strain appears to be more promising as a tool for xenotransplantion of human tumors. However, the NOD-SCID mouse strain retains natural killer (NK) cell activity, macrophage function, complement activity and functional dendritic cells.[13] NK cells might play an important role in the rejection of implanted tissues or cells in SCID mice.[14–17] Although several models using mainly conventional nude and SCID mice are available, there are some major drawbacks: the requirement of long time periods, repeated transplantation, total body irradiation of mice, hormone supplements, etoposide pretreatment and anti-NK monoclonal antibodies required for tumor formation. These problems appear to hinder wider use of these animal models. Due to the low engraftment efficiency of hematopoietic and tumor cells transplanted in SCID mice, T, B and NK knock-out NOD/SCID/γc^{null} (NOG) mice were used in the present study to investigate the role of NK in tumor growth and metastasis.[13]

Natural killer cells are a type of lymphocyte that comprises up to 15% of peripheral blood lymphocytes and mediates innate immunity against pathogens and tumors.[17] In addition, NK cells are an important source of cytokines that regulate hematopoiesis and link the innate to the adaptive immune response through a bidirectional cross-talk with dendritic cells.[18,19] NK cells were originally discovered because of their ability to kill tumor and virally infected cells *in vitro*. NK-cell activity against these *in vitro* targets is spontaneous; it is readily apparent in individuals who have not been previously exposed to the target cell antigens. A clear involvement of NK cells in antitumor immunity *in vivo*, and the involvement of major histocompatibility complex (MHC) class I in NK-cell recognition, was shown in 1986 by Karre and colleagues.[20] They showed that the RMA T-cell lymphoma, derived from the Rauscher virus-induced murine cell line RBL-5, grew progressively in syngenic mice, but that an MHC class I-negative variant, RMA-S, was rejected by host NK cells. In many different situations, NK cells were shown to kill certain tumor cell lines *in vitro*, despite significant levels of MHC class I on their cell surface.[21,22] This implied that killing of MHC class I^+ tumor cells was mediated by activating receptors that were either not impaired by the inhibitory NK receptors for MHC class I or provided sufficient stimulation to overcome the negative regulation.

One cohort study showed that individuals with low natural cytotoxic activity of peripheral blood lymphocytes are at a

[9]To whom correspondence should be addressed. E-mail: yamamoto.mmb@tmd.ac.jp

doi: 10.1111/j.1349-7006.2006.00319.x

significantly higher risk of cancer, compared with those of median or high activity.[23] It has been reported recently that NK cells isolated from HIV-infected individuals are impaired in their ability to kill the virus-infected autologous cells, as well as tumor cell lines.[24–27] Previous studies also reported that NK-cell activity controls PEL and Kaposi's sarcoma (KS) development associated with HHV-8 infection.[28,29] The ability of the NK cells to kill relevant targets, such as tumor or virally infected cells, depends on the delicate balance of the patterns of expression of MHC class I-specific inhibitory NK receptors and activating receptors.[30,31] As there is no animal model in which NK-cell activities are genetically and selectively deficient to rule out the function of NK cells in viral infection and tumor growth and metastasis, most studies have relied on depleting NK cells in mice using monoclonal or polyclonal antibodies.[32,33] Depletion of NK cells *in vivo* by anti-NK antibody leads to enhanced tumor formation in several mouse tumor models.[15,34] Therefore, the role of NK cells in the course of tumor growth and infiltration as well as viral infection remains one of the major topics in tumor immunology.

In the present study, we investigated the direct involvement of NK cells in growth and infiltration of PEL cells using T, B and NK knock-out NOG mice,[13,35,36] and T and B knock-out NOD/SCID mice. NK knock-out NOG mice were most efficient in the formation of large tumors, massive ascites and infiltration within 3 weeks in comparison with NK-bearing NOD/SCID mice. We also provide evidence that activated human NK cells inhibit tumor growth and infiltration in NOG mice. These results suggest that NK cells play an important role in tumor growth and infiltration, and activated NK cells could be a promising immunotherapeutic strategy against AIDS-associated PEL or other malignancies either alone or in combination with conventional therapy.

Materials and Methods

Mice and inoculation of cell lines. NOG and NOD/SCID mice were obtained from the Central Institute for Experimental Animals (Kawasaki, Japan). All mice were maintained under specific pathogen-free conditions at the Animal Center of Tokyo Medical and Dental University (Tokyo, Japan). The Ethical Review Committee of the institute approved the experimental protocol.

Primary effusion lymphoma cell lines BCBL-1[37] and TY-1,[38] NK cell line KHYG-1 and bcr-abl$^+$ leukemic cell line K562 were cultured in RPMI-1640 medium supplemented with 2% heat-inactivated fetal bovine serum (FBS; JRH Biosciences, Lenexa, KS, USA), 100 U/mL penicillin and 10 μg/mL streptomycin. BCBL-1 and TY-1 cells were washed twice with serum-free RPMI-1640 and resuspended in fresh RPMI-1640. Mice were anesthetized with ether and cells were inoculated either subcutaneously (sc) in the postauricular region or intraperitoneally (ip) in the abdominal region of mice at doses of 1×10^7 and 2×10^6 cells per mouse, respectively. BCBL-1 cells were also inoculated either sc in the postauricular region or ip in the abdominal region of NOD/SCID mice with or without pretreatment with TMβ1 antibody, or in NOG mice. All mice were killed 3 weeks after inoculation with PEL cells. We measured tumor size, collected ascites from the abdomen of mice, and measured the volume of ascites.

Isolation and culture of NK cells. Blood was collected after obtaining informed consent from healthy volunteers. Peripheral blood mononuclear cells (PBMC) were isolated from the blood by Ficoll-Hypaque gradient centrifugation (Amersham Biosciences, Uppsala, Sweden), washed twice with RPMI-1640, and the number of cells counted. To generate activated NK cells, PBMC were cultured in anti-CD16-coated flasks with AIM-V medium (Invitrogen, Tokyo, Japan) supplemented with 5% auto-plasma, 700 U/mL interleukin (IL)-2 (Chiron, Amsterdam, the Netherlands), and 1 μL/mL OK432 (Chugai Pharmaceutical, Tokyo, Japan) for 24 h at 39°C, and then the cultured cells were centrifuged at 550 *g* for 10 min and the supernatants were discarded. Cells were again cultured in anti-CD16-uncoated flasks with AIM-V medium supplemented with 5% auto-plasma, and 700 U/mL IL-2 at 37°C for 2–3 weeks. During culture periods, we added medium several times for expansion and maintenance of activated NK cells. The purity of NK cells was 92–95%.

Flow cytometric analysis and cytotoxic activity. For five-color flow cytometric analysis (Cytomics FC500; Beckman Coulter, Miami, FL, USA), freshly isolated and activated NK cells were stained with monoclonal antibodies (ECD-labeled anti-CD3, PC5-labeled anti-CD4, PC7-labeled anti-CD8, PC7-labeled anti-CD16, PE or PC7-labeled anti-CD45, PC5-labeled anti-CD56, and PE-labeled anti-CD69 [Immunotech, Marseile, France]) and appropriate anti-isotypic monoclonal antibodies stained as negative controls. Data were analyzed by using CXP Analysis software version 1.1.

Freshly isolated and activated NK cells were tested for cytotoxic activity at various effector-to-target (E/T) ratios in a calcein-AM release assay using TERASCAN VP (Minerva Tech., Tokyo, Japan). We labeled the target cells with the immunofluorescent dye Calcein-AM solution (Do Jindo Laboratory, Kumamoto, Japan) and incubated them for 30 min. The cells were then washed with phosphate-buffer saline (PBS)(–) and the fluorescence intensity checked. Target cells and effector cells were suspended in RPMI-1640 with 10% FBS at various E/T ratios, added into 96-well plates and incubated for 2 h, and the fluorescence intensity was again checked.

Inoculation of activated NK cells into mice and collection of samples. Mice were inoculated with BCBL-1 (2×10^6) cells ip in the abdominal region of NOG mice. Three days after inoculation of PEL cells, mice were treated with either RPMI-1640 (control mice) or activated NK cells (1×10^7) ip on days 4, 10 and 17. All mice were killed 3 weeks after inoculation with PEL cells. We measured tumor size, collected ascites from the abdomen of mice, and measured the volume of ascites. Tissues and various organs of mice were also collected and fixed with 10% buffered formalin (Streck Tissue Fixative, Omaha, NE, USA), then processed to paraffin-embedded sections for staining with hematoxylin and eosin (HE) and immunostaining.

Immunohistochemistry. Paraffin sections of various organs were deparaffinized and hydrated in xylene or clearing agents and a graded alcohol series, then rinsed for 5 min in water. Deparaffinized samples were incubated with 0.025% trypsin/PBS for 30 min followed by washing, and then incubated with 0.3% H_2O_2 in methanol for 30 min at room temperature before being washed twice with PBS. Immunostaining was done for PEL cells with a 1:500 dilution of primary rabbit polyclonal antibody specific for HHV-8-encoded LANA.[39] This was followed by washing in PBS and incubation with a secondary antibody, biotinylated antirabbit IgG, after which cells were again washed in PBS and incubated with horseradish peroxidase-conjugated streptavidin for 30 min at room temperature. After two washes in PBS, the amplification procedure was carried out using kits according to the manufacturer's instructions (catalyzed signal amplification system kit; DAKO, Copenhagen, Denmark). The signal was visualized using 0.2 mg/mL diaminobenzidine and 0.015% H_2O_2 in 0.05 M Tris-HCl, pH 7.6. Positive staining was visualized after incubation of these samples with a mixture of 0.05% 3,3′-diaminobenzidine tetrahydrochloride in 50 mM Tris-HCl buffer and 0.01% H_2O_2 for 5 min. The samples were counterstained with hematoxylin for 2 min, dehydrated completely, cleaned in xylene and then mounted. HE and immunostaining were visualized and photographed under light microscopy (BX41 and DP70; Olympus, Tokyo, Japan).

doi: 10.1111/j.1349-7006.2006.00319.x

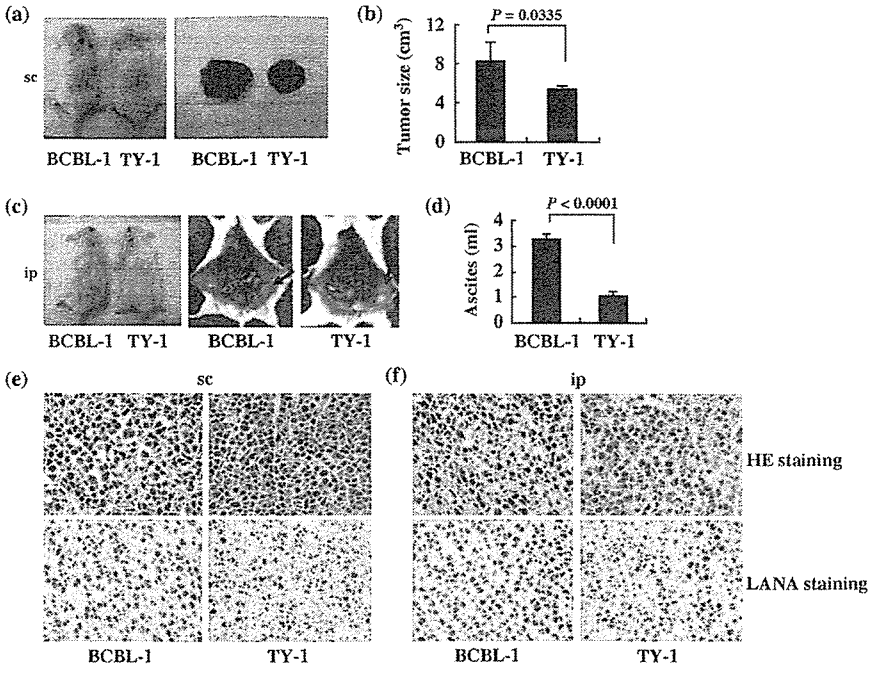

Fig. 1. Successful engraftment and tumor marker of primary effusion lymphoma (PEL) cells in T, B and natural killer (NK) knock-out NOG mice. (a) Photograph of mice inoculated with BCBL-1 and TY-1 cells subcutaneously in the postauricular region (left panel) and those of subcutaneously formed BCBL-1 and TY-1 tumor 3 weeks after inoculation of cells (right panel). (b) Subcutaneous tumor size of mice inoculated with BCBL-1 and TY-1 cells, shown as the mean ± s.e.m. from five mice ($P = 0.0335$). (c) Photograph of ascites-bearing mice inoculated with BCBL-1 and TY-1 cells intraperitonealy in the abdominal region (left panel) and peritoneal cavity of mice 21 days after inoculation of BCBL-1 (middle panel) and TY-1 cells (right panel). Arrow head indicates the tumor in mice inoculated intraperitonealy. (d) Volume of ascites in mice inoculated with various BCBL-1 and TY-1 cells, shown as the mean ± s.e.m. from five mice ($P < 0.0001$). (e,f) Hematoxylin–eosin (HE) and immunohistochemical staining of tumor tissue of BCBL-1 and TY-1 cells injected mice. Upper panels represent HE staining. Immunohistochemical staining was conducted using rabbit anti-LANA (lower panels). Left and right panels represent results with BCBL-1 and TY-1, respectively (magnification, ×40). Data are from (e) mice inoculated subcutaneously and (f) mice inoculated intraperitonealy.

Statistical analysis. The statistical analysis was carried out using StatView J-4.5 (Hulinks, Tokyo, Japan).

Results

Rapid tumor and massive ascites formation and infiltration of PEL cells in T, B and NK knock-out NOG mice. To investigate *in vivo* growth, PEL cell lines (BCBL-1 and TY-1) were inoculated sc in the postauricular region of NOG mice (Fig. 1a,b). Mice inoculated with cell lines BCBL-1 and TY-1 produced a visible tumor within 3 weeks in all NOG mice. The BCBL-1 cell line was very efficient in the formation of a large tumor (Fig. 1a,b), as well as development of clinical signs of near-death, such as pilorection, weight loss and cachexia in mice at the time of killing. The average tumor size in NOG mice inoculated with BCBL-1 and TY-1 was 8.25 cm^3 and 5.43 cm^3, respectively. PEL is an AIDS-associated non-Hodgkin's lymphoma that is characterized by lymphomatous effusions of serous cavities and rarely presents with a definable tumor mass.[5,7] To establish a clinically relevant PEL model, we inoculated BCBL-1 and TY-1 cells ip in the abdominal region of NOG mice (Fig. 1c,d). BCBL-1 and TY-1 produced massive ascites and a small tumor mass in the peritoneal cavity within 3 weeks of inoculation in all mice. The BCBL-1 cell line was most efficient in the formation of massive ascites (Fig. 1c,d), as well as development of clinical signs of near-death. The average volume of ascites in NOG mice inoculated with BCBL-1 and TY-1 was 3.26 mL and 1.05 mL, respectively. To test whether tumors maintain original histomorphology and expression patterns of tumor markers in NOG, we carried out HE and immunostaining of tumor tissues and various organs obtained from mice inoculated with BCBL-1 and TY-1 cells. Histological and immunological analysis revealed that *in vivo* tumor cells had well-preserved morphology as well as expression of the viral gene *LANA* (Fig. 1e,f). These results show that PEL cell lines inoculated either sc into the postauricular region or ip in the abdominal region of NOG mice were able to produce a large tumor and ascites very efficiently. Interestingly, ip-inoculated PEL cells were found to form clinically relevant lymphomatous effusions in the peritoneal cavity as well as a small definable mass.

To assess the tissue distribution of PEL cells, we carried out histological examinations of the different organs of NOG mice after inoculation of the cells. Infiltration of tumor cells was found not only in primary tumor tissues, but also to a lesser extent in the lung of NOG mice inoculated sc with BCBL-1 and TY-1 (Fig. 2a,b). We found that mice inoculated ip with BCBL-1 cells exhibited infiltration in the lung, liver and spleen (Fig. 2c), whereas TY-1 cells did so to a lesser extent only in the lung and liver (Fig. 2d). HE and immunohistochemical staining showed a degree of infiltration of tumor cells at the site of inoculation and various organs with BCBL-1 and TY-1 (Fig. 2). Furthermore, BCBL-1 was most efficient at infiltrating the lung (Fig. 2a,c). Interestingly, ip-inoculated PEL cells appeared to infiltrate various organs of mice more aggressively and massively than sc inoculation. This extremely rapid tumor formation and infiltration in all mice is one of the hallmarks of our clinically relevant animal model without changes in histomorphology or tumor marker expression.

Role of NK cells in the growth and infiltration of PEL cell *in vivo*. Severe combined immunodeficiency mice lack functional T and B lymphocytes, but NK-cell activity remains normal.[10,17,40] Despite severe immunological defects, SCID mice have the ability to reject xenografts. Further, immunosupression of SCID by treatment with etoposide, irradiation or an anti-NK antibody, which transiently abrogates NK-cell activity *in vivo*, results in enhanced tumor growth in mice.[41–47] To determine the possibility that NK-cell activity suppresses tumorigenesis in conventional SCID mice, the PEL cell line BCBL-1 was inoculated either sc in the postauricular region or ip in the abdominal region of T and B knock-out NOD/SCID mice with or without pretreatment of with TMβ1 antibody, or T, B and NK knock-out NOG mice (Fig. 3a–g). BCBL-1 cells were able to produce tumors at inoculation sites in NOD/SCID mice with common γ-chain. Immunosupression of NOD/SCID by treatment with an antimurine TMβ1 antibody, which transiently abrogates natural killer cell activity *in vivo*, resulted in induction of larger tumor and ascites formation in comparison with non-treated NOD/SCID mice. NOG mice lacking common γ-chain inoculated with BCBL-1 cells were most efficient in the formation of large tumor and massive ascites within 3 weeks.

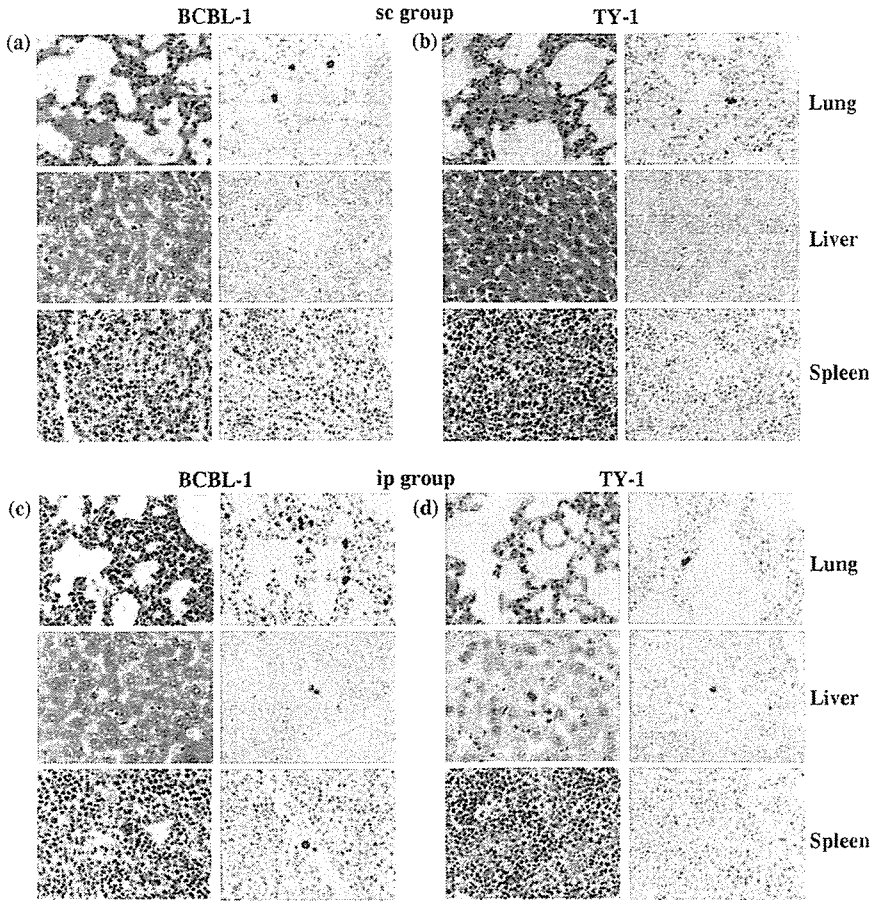

Fig. 2. Metastasis of primary effusion lymphoma (PEL) cells in various organs of T, B and natural killer (NK) knock-out NOG mice. (a–d) Histological analysis of lung, liver and spleen of mice inoculated with BCBL-1 and TY-1 cells either (a,b) subcutaneously (sc) or (c,d) intraperitonealy (ip). Immunohistochemical staining was conducted using anti-LANA. Data are from (a,c) BCBL-1-inoculated mice and (b,d) TY-1-inoculated mice. Left and right panels of all figures represent hematoxylin–eosin and immunostaining, respectively (magnification, ×40).

NOG mice have a defective common cytokine receptor, γ chain. Mutation in the common cytokine receptor γ chain leads to life-threatening, X-linked, severe combined immunodeficiency disease (XSCID) in humans, characterized by an extremely low number of T and NK cells.[48,49] These results suggest that NK cells are responsible for the formation of a progressively growing rapid large tumor and massive ascites of PEL cells in SCID mice at inoculation sites.

Severe combined immunodeficiency mice have NK cells, an important immune effector population implicated in protection against tumor metastasis and viral infection.[17,50] It has been reported recently that individuals with low natural cytotoxic activity of peripheral blood lymphocytes are at a significantly higher risk of cancer, compared with those of median or high activity, as well as functional impairment of NK cells in viral infection.[23] To assess the infiltration of PEL cells, we carried out histological examinations of tumor tissue and the different organs of mice inoculated with BCBL-1 cells (Fig. 3h). Infiltration of tumor cells was found in various organs of NOG mice inoculated with BCBL-1 cells. We found that NOD/SCID inoculated with BCBL-1 cells exhibited no infiltrate in any organs. NOD/SCID mice immunosuppressed by pretreatment with anti-NK antibody showed infiltration of PEL cells to a lesser extent in various organs of mice inoculated with BCBL-1 cells. HE and immunohistochemical staining showed a degree of infiltration of tumor cells in the lung of mice inoculated with BCBL-1 (Fig. 3h). These results suggest that NK cells play an important role in the infiltration of cancer cells in various organs.

Activated NK cells inhibit tumor growth and infiltration *in vivo*. As the above results suggested the potential role of NK cells in tumor growth and metastasis, we next examined whether adoptive transfer of activated NK cells could inhibit tumor growth and infiltration of xenografted PEL cells in the NOG mouse model. For this purpose, freshly isolated PBMC from the blood of healthy donors were cultured for 2–3 weeks to generate NK cells. NK cells were expanded *ex vivo* by several hundred to 2500-fold after 2 weeks cultivation and the expression level of CD69, an activated marker of NK cells, was increased dramatically. The purity of the activated NK cells used in the present study was 92–95% (data not shown). NK cells use cytoplasmic granules containing perforins and granzymes to kill the target cells. Using a highly sensitive flow cytometry-based intracellular cytokine assay, we next investigated the expression of intracellular perforins and granzymes in NK cells. Intracellular perforin and granzyme expression was increased in activated culture cells in comparison to freshly isolated cells from healthy donors (data not shown). PBMC, NK cell line KHYG-1 and activated NK cells were analyzed for cytotoxic activity against the NK-susceptible K562 erythroleukemia cell line (Fig. 4a,b). Cytotoxic activity of cells cultured for 2 weeks was increased significantly compared with freshly isolated PBMC from healthy donors (Fig. 4b). Activated NK cells also killed PEL cells efficiently *in vitro* at various E/T ratios, but the NK cell line KHYG-1 did not (Fig. 4c).

To examine the antitumor effect of activated NK cells against PEL, we injected the PEL cell line BCBL-1 (2×10^6) ip into the abdominal region of NOG mice. Three days after inoculation, mice were treated with either RPMI-1640 (as control) or activated NK cells (1×10^7) ip on days 4, 10 and 17. BCBL-1 cell inoculation promoted the development of massive ascites in the peritoneal cavity of all control mice within 3 weeks of inoculation. In contrast, activated NK-treated mice appeared to be

doi: 10.1111/j.1349-7006.2006.00319.x

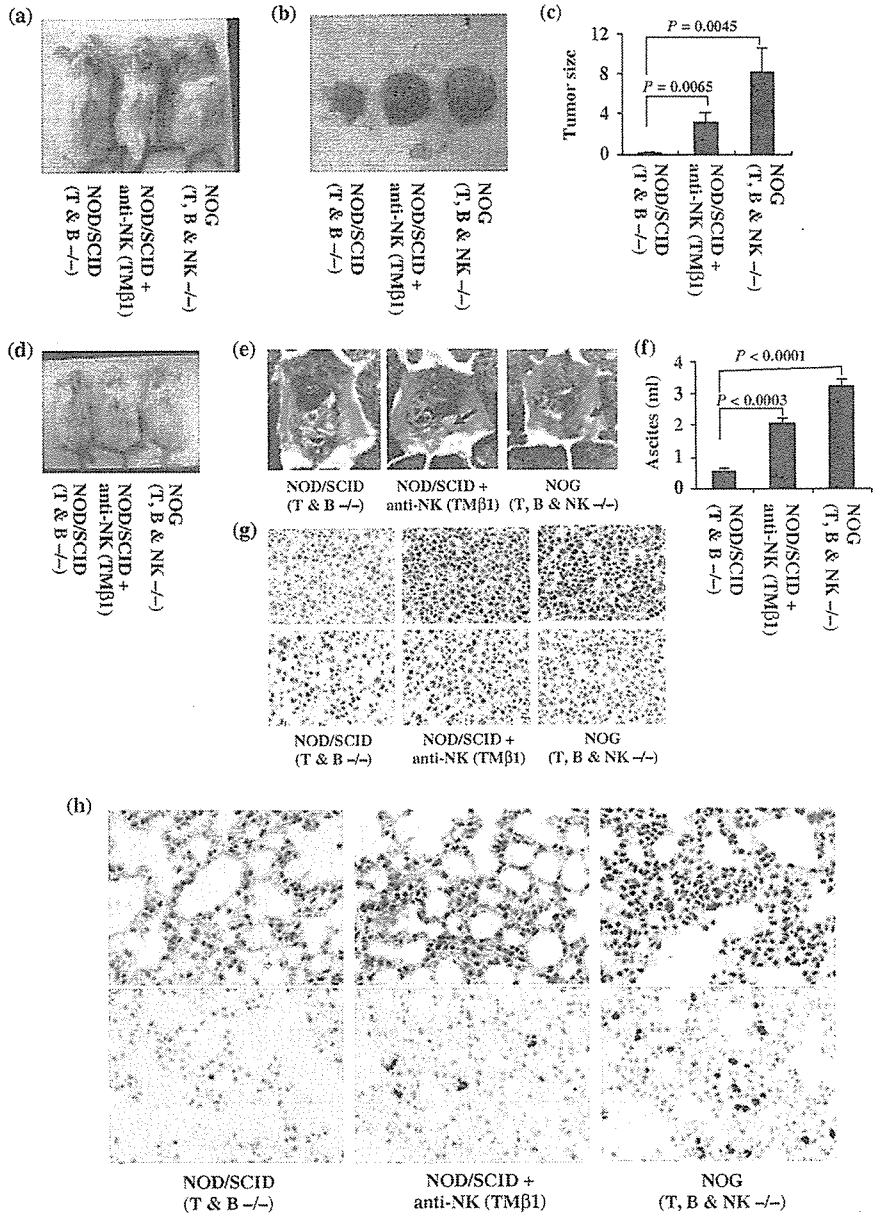

Fig. 3. Natural killer (NK) cells in tumor growth and infiltration. BCBL-1 cells were inoculated subcutaneously in the postauricular region or intraperitonealy in the abdominal region of T and B knock-out NOD/SCID, TMβ1-pretreated T and B knock-out NOD/SCID and T, B and NK knock-out NOG mice. (a) Photograph of mice inoculated with BCBL-1 cells subcutaneously in the postauricular region. (b) Photograph of BCBL-1 tumor 3 weeks formed subcutaneously after inoculation of cells. (c) Subcutaneous tumor size of mice inoculated with BCBL-1 cells, shown as the mean ± s.e.m. from six mice. Tumor size of TMβ1-pretreated NOD/SCID mice was significantly larger than NOD/SCID ($P = 0.0065$) and that of NOG mice was more significant than NOD/SCID ($P = 0.0045$). (d) Photograph of ascites-bearing mice inoculated with BCBL-1 cells intraperitonealy in the abdominal region. (e) Photograph of the peritoneal cavity of mice 3 weeks after inoculation of BCBL-1. Left, middle and right panels represent the T and B knock-out NOD/SCID, TMβ1-pretreated T and B knock-out NOD/SCID and T, B and NK knock-out NOG mice, respectively. Arrow head indicates the tumor in mice inoculated intraperitonealy. (f) Volume of ascites in mice inoculated with BCBL-1 cells, shown as the mean ± s.e.m. from six mice. Volume of ascites in TMβ1-pretreated NOD/SCID mice was significantly higher than NOD/SCID ($P = 0.0003$) and that of NOG mice was more significant than NOD/SCID ($P < 0.0001$). Hematoxylin–eosin (HE) and immunohistochemical staining of (g) lung tissue and (h) tumor tissue of BCBL-1-injected mice. Upper panels represent HE staining. Immunohistochemical staining was conducted using rabbit anti-LANA (lower panels). Left, middle and right panels represent results from T and B knock-out NOD/SCID, TMβ1-pretreated T and B knock-out NOD/SCID and T, B and NK knock-out NOG mice, respectively. Magnification, ×40.

healthy and had a significantly lower volume of ascites (Fig. 5a,b). Clinical evaluation of organ infiltration 3 weeks after injection of PEL cells showed that activated NK treatment inhibited their infiltration into the lung. In contrast, all control mice showed massive infiltration of tumor cells into the lung (Fig. 5c). Organ infiltration of tumor cells was analyzed and evaluated by HE and immunostaining of LANA. These data indicate that activated NK cells significantly inhibit the growth and infiltration of PEL cells *in vivo* (Fig. 5).

Discussion

Natural killer cells form a first line of defense against pathogens or host cells that are stressed or cancerous. To execute the concept of using activated NK cells in order to prevent cancer, it is indispensable to know how NK cells are important for tumor growth and infiltration. There have been a number of reports about the contribution of NK cells in tumor growth and metastasis. In particular, whole-body irradiation has been reported to suppress NK activity and increase the ability of human and murine tumors to be transplanted into SCID mice.[42–46] Treatment of mice with murine anti-NK antibody, which transiently inhibits NK-cell activity, results in efficient engraftment of tumor cells in SCID mice.[15,47] In the present study, we demonstrated the direct role of NK cells in tumor growth and metastasis using T, B and NK knock-out NOG and T and B knock-out NOD/SCID mice. PEL cells were able to produce a large tumor and massive ascites very efficiently at inoculated sites and infiltrate various organs in T, B and NK nock-out NOG mice. We found that T and B knock-out NOD/SCID mice inoculated with PEL cells formed small tumors and a lower volume of ascites, but completely failed to infiltrate. T and B knock-out NOD/SCID mice were further immunosuppressed by pretreatment with anti-NK antibody, which enhanced tumor and ascites formation as well as organ infiltration. These results demonstrate the critical role of NK cells in tumor growth and infiltration using NK knock-out mice. It is of particular importance that ip-inoculated PEL cells were found to form clinically relevant lymphomatous effusions in the peritoneal cavity and small tumor mass as well as infiltration. This clinically relevant

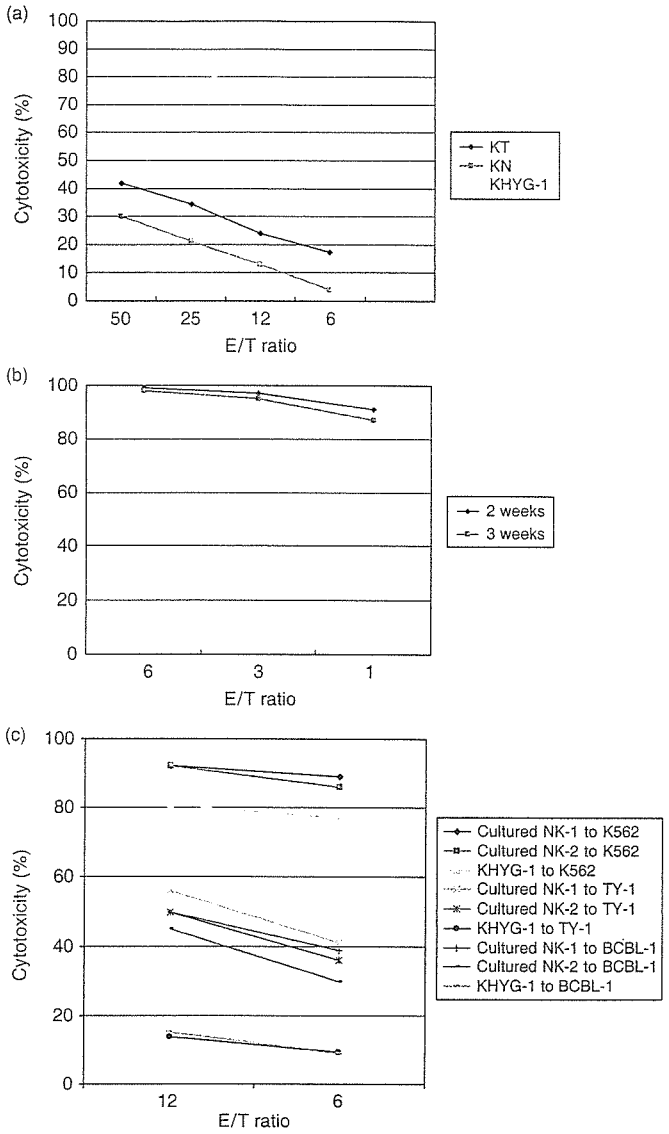

Fig. 4. Cytotoxic activity of activated natural killer (NK) *in vitro* culture cells. (a) Spontaneous cytotoxic activity of freshly isolated peripheral blood mononuclear cells (KT-1 and KN-2 represent samples from two donors) and NK cell line KHYG-1 against K-562 cells at different effector-to-target (E/T) ratios. (b) Cells cultured for 2 weeks against K-562 cells at different E/T ratios. (c) Cytotoxic activity of activated NK cells (NK-1 and NK-2 represent samples from two donors) against primary effusion lymphoma cells *in vitro* at various E/T ratios.

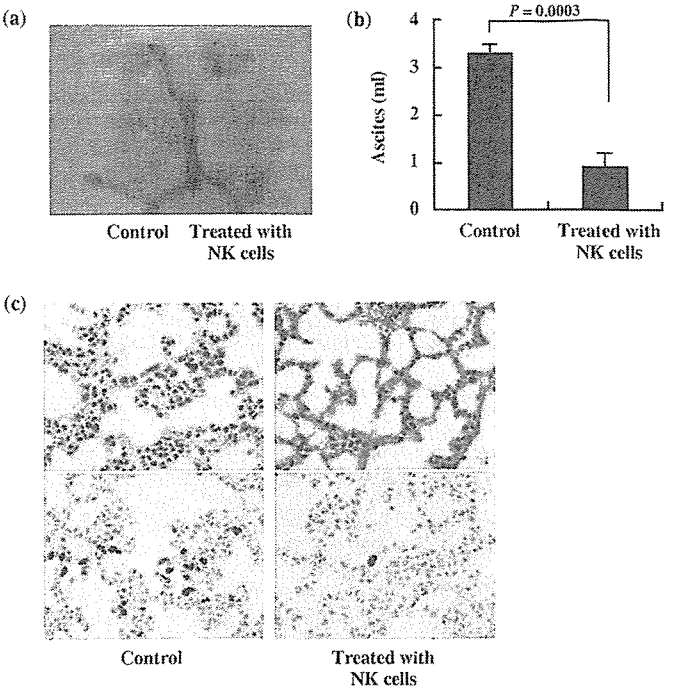

Fig. 5. Inhibition of primary effusion lymphoma (PEL) cell growth and infiltration in NOG mice. T, B and natural killer (NK) knock-out NOG mice were injected with PEL cells (2×10^6) intraperitonealy in the abdominal region. Mice were administered either RPMI-1640 or activated NK cells (1×10^7) intraperitonealy on days 4, 10 and 17 followed by observation for up to 3 weeks. (a) Photograph of ascites-bearing control PEL mice and activated NK-treated PEL mice. (b) Volume of ascites in control PEL mice and activated NK-treated PEL mice. Volume of ascites in mice inoculated with BCBL-1 cells, shown as the mean ± s.e.m. from six mice ($P = 0.0003$). (c) Hematoxylin–eosin (HE) and immunohistochemical staining of the lung of NOG mice 3 weeks after inoculation of PEL cells using anti-LANA. Upper and lower panels show HE and immunohistochemical staining, respectively. Left and right panels represent the data from control mice and mice treated with activated NK cells, respectively. Magnification, ×40. The data represent six mice in each group and three healthy donors (two mice for each donor).

animal model without changes in its histomorphology or tumor marker expression would be useful to understand and investigate the mechanism of PEL cell growth and infiltration.

In patients with cancer and viral infection, NK-cell function has been shown to be impaired, as determined by the reduced proliferation, response to interferon (IFN), and cytotoxicity of the cells of patients *ex vivo*.[51,52] In the present study, we inoculated activated NK cells to treat tumor-bearing mice to further clarify the role of NK cells in tumor growth and infiltration. Transfer of activated NK cells in T, B and NK knock-out NOG mice showed significant inhibition of tumor and ascites formation as well as infiltration. T, B and NK knock-out NOG mice treated with activated NK cells rejected the tumor cells to a similar extent as T and B knock-out NOD/SCID mice.

Natural killer cells kill target cells by various mechanisms. One way is by the release of cytoplasmic granules – complex organelles that combine specialized storage and secretory functions with the generic degradative functions of lysosomes. These granules contain a number of proteins, such as perforins and granzymes, which lyse target cells. Increased perforin and granzyme expression in activated NK cells was significantly correlated with inhibition of tumor growth and metastasis in the NOG mouse model. Perforin- and granzyme-mediated apoptosis is the principal pathway used by NK cells to eliminate tumor and virus-infected cells.[53] Studies in perforin-deficient mice have revealed that this protein is required for most NK-cell cytotoxicity.[54]

In summary, NK knock-out NOG mice were very efficient in the formation of primary tumors and organ infiltration. These results indicate that activated human NK cells prevent tumor growth and infiltration in NOG mice. Finally, our results suggest that NK cells play a critical role in tumor growth and infiltration, and that activated NK cells could be a promising immunotherapeutic strategy against cancer or viral infection either alone or in combination with conventional therapy. The reproducible growth behavior and preservation of characteristic features of PEL cells also suggest that the NOG mouse model system described in the present study may provide a novel opportunity to understand and investigate the mechanism of pathogenesis and malignant cell growth of PEL.

doi: 10.1111/j.1349-7006.2006.00319.x

Acknowledgments

We thank K. Ohba of the Department of Molecular Virology, S. Ichinose of the Instrumental Analysis Research Center and S. Endo of the Animal Research Center, Tokyo Medical and Dental University for their advice and assistance with the experiments. We also thank Y. Sato of the National Institute of Infectious Diseases for her excellent technical assistance. This work was supported by grants from the Ministry of Education, Science and Culture; the Ministry of Health, Labor and Welfare; and Human Health Science of Japan.

References

1 Jaffe ES, Harris NL, Stein H, Vardiman JW, eds. *World Health Organization Classification of Tumors, Pathology and Genetics of Tumors of Haematopoietic and Lymphoid Tissues*. Lyon, France: IARC Press, 2001.
2 Gaidano G, Carbone A. Primary effusion lymphoma: a liquid phase lymphoma of fluid-filled body cavities. *Adv Cancer Res* 2001; **80**: 115–46.
3 Cesarman E, Knowles DM. The role of Kaposi's sarcoma-associated herpesvirus (KSHV/HHV-8) in lymphoproliferative diseases. *Semin Cancer Biol* 1999; **9**: 165–74.
4 Klein U, Gloghini A, Gaidano G *et al.* Gene expression profile analysis of AIDS-related primary effusion lymphoma (PEL) suggests a plasmablastic derivation and identifies PEL-specific transcripts. *Blood* 2003; **102**: 4115–21.
5 Cesarman E, Chang Y, Moore PS, Said JW, Knowles DM. Kaposi's sarcoma-associated herpesvirus-like DNA sequences in AIDS-related body-cavity-based lymphomas. *N Engl J Med* 1995; **332**: 1186–91.
6 Horenstein MG, Nador RG, Chadburn A *et al.* Epstein–Barr virus latent gene expression in primary effusion lymphomas containing Kaposi's sarcoma-associated herpesvirus/human herpesvirus-8. *Blood* 1997; **90**: 1186–91.
7 Nador RG, Cesarman E, Chadburn A *et al.* Primary effusion lymphoma: a distinct clinicopathologic entity associated with the Kaposi's sarcoma-associated herpes virus. *Blood* 1996; **88**: 645–56.
8 Schmidt M, Deschner EE, Thaler HT, Clemments L, Good RA. Gastrointestinal cancer studies in the human to nude mouse heterotransplant system. *Gastroenterology* 1977; **72**: 829–37.
9 Bosma GC, Custer RP, Bosma MJ. A severe combined immunodeficiency mutation in the mouse. *Nature* 1983; **301**: 527–30.
10 Schuler W, Bosma MJ. Nature of the scid defect: a defective VDJ recombinase system. *Curr Top Microbiol Immunol* 1989; **152**: 55–62.
11 Kamel-Reid S, Letarte M, Sirard C *et al.* A model of human acute lymphoblastic leukemia in immune-deficient SCID mice. *Science* 1989; **246**: 1597–600.
12 Mosier DE, Gulizia RJ, Baird SM, Wilson DB. Transfer of a functional human immune system to mice with severe combined immunodeficiency. *Nature* 1988; **335**: 256–9.
13 Ito M, Hiramatsu H, Kobayashi K *et al.* NOD/SCID/γc^{null} mouse: An excellent recipient mouse model for engraftment of human cells. *Blood* 2002; **100**: 3175–82.
14 Dorshkind K, Pollack SB, Bosma MJ, Phillips RA. Natural killer (NK) cells are present in mice with severe combined immunodeficiency (scid). *J Immunol* 1985; **134**: 3798–801.
15 Feuer G, Stewart SA, Baird SM, Lee F, Feuer R, Chen ISY. Potential role of natural killer cells in controlling tumorigenesis by human T-cell leukemia Viruses. *J Virol* 1994; **69**: 1328–33.
16 Welsh RM. Regulation of virus infections by natural killer cells: a review. *Nat Immun Cell Growth Regul* 1986; **5**: 169–99.
17 Trinchieri G. Biology of natural killer cells. *Adv Immunol* 1989; **47**: 187–376.
18 Moretta A. Natural killer cells and dendritic cells: rendezvous in abused tissues. *Nat Rev Immunol* 2002; **2**: 957–64.
19 Raulet DH. Interplay of natural killer cells and their receptors with the adaptive immune response. *Nat Immunol* 2004; **5**: 996–1002.
20 Karre K, Ljungger HG, Piontek G, Kiessling R. Selective rejection of H-2-deficient lymphoma variants suggests alternative immune defense strategy. *Nature* 1986; **319**: 675–8.
21 Pena J, Alonso C, Solana R, Serrano R, Carracedo J, Ramirez R. Natural killer susceptibility is independent of HLA class I antigen expression on the cell lines obtained from human solid tumors. *Eur J Immunol* 1990; **20**: 2445–9.
22 Litwin V, Gumperz J, Parham P, Philips JH, Lanier LL. Specificity of HLA class I antigen recognition by human NK clones: evidence for clonal heterogeneity, protection by self and non-self alleles, and influence of the target cell type. *J Exp Med* 1993; **178**: 1321–36.
23 Imai K, Matsuyama S, Miyake S, Suga K, Nakachi K. Natural cytotoxic activity of peripheral-blood lymphocytes and cancer incidence: an 11-year follow-up study of a general population. *Lancet* 2000; **356**: 1795–9.
24 Ullum H, Gotzsche PC, Victor J, Dickmeiss E, Skinhoj P, Pedersen BK. Defective natural immunity: an early manifestation of human immunodeficiency virus infection. *J Exp Med* 1995; **182**: 789–99.
25 Ahmad R, Menezes J. Defective killing activity against gp120/41-expressing human erythroleukaemic K562 cell line by monocytes and natural killer cells from HIV-infected individuals. *AIDS* 1996; **10**: 143–9.
26 Scott-Algara D, Paul P. NK cells and HIV infection: lessons from other viruses. *Curr Mol Med* 2002; **2**: 757–68.
27 Bonaparte MI, Barker E. Inability of natural killer cells to destroy autologous HIV-infected T lymphocytes. *AIDS* 2003; **17**: 487–94.
28 Sirianni MC, Libi F, Campagna M *et al.* Downregulation of the major histocompatibility complex class I molecules by human herpesvirus type 8 and impaired natural killer cell activity in primary effusion lymphoma development. *Br J Haematol* 2005; **130**: 92–5.
29 Sirianni MC, Vincenzi L, Topino S *et al.* NK cell activity controls human herpesvirus 8 latent infection and is restored upon highly active antiretroviral therapy in AIDS patients with regressing Kaposi's sarcoma. *Eur J Immunol* 2002; **32**: 2711–20.
30 Lanier LL. NK cell receptors. *Annu Rev Immunol* 1998; **16**: 356–93.
31 Moretta A, Bottino C, Mingari MC, Biassoni R, Moretta L. What is a natural killer cell? *Nat Immunol* 2002; **3**: 6–8.
32 Koo GC, Dumont FJ, Tutt M, Hackett J Jr, Kumar V. The NK-1.1(–) mouse: a model to study differentiation of murine NK cells. *J Immunol* 1986; **137**: 3742–7.
33 Smyth MJ, Crowe NY, Godfrey DI. NK cells and NKT cells collaborate in host protection from methylcholanthrene-induced fibrosarcoma. *Int Immunol* 2001; **13**: 459–63.
34 Smyth MJ, Godfery DI, Trapani JA. A fresh look at tumor immunosurveillance and immunotherapy. *Nature* 2001; **2**: 293–9.
35 Dewan MZ, Terashima K, Taruishi M *et al.* Rapid tumor formation of human T-cell leukemia virus type 1-infected cell lines in novel NOD-SCID/γc^{null} mice: suppression by an inhibitor against NF-κB. *J Virol* 2003; **77**: 5286–94.
36 Dewan MZ, Uchihara JN, Terashima K *et al.* Efficient intervention of growth and infiltration of primary adult T-cell leukemia cells by an HIV protease inhibitor, ritonavir. *Blood* 2006; **107**: 716–24.
37 Renne R, Zhong W, Herndier B *et al.* Lytic growth of Kaposi's sarcoma-associated herpesvirus (human herpesvirus 8) in culture. *Nat Med* 1996; **2**: 342–6.
38 Katano H, Hoshino Y, Morishita Y *et al.* Establishing and characterizing a CD30-positive cell line harboring HHV-8 from a primary effusion lymphoma. *J Med Virol* 1999; **58**: 394–401.
39 Katano H, Sato Y, Kurata T, Mori S, Sata T. High expression of HHV-8-encoded ORF73 protein in spindle-shaped cells of Kaposi's sarcoma. *Am J Pathol* 1999; **155**: 47–52.
40 Dorshkind K, Pollack SB, Bosma MJ, Phillips RA. Natural killer (NK) cells are present in mice with severe combined immunodeficiency (scid). *J Immunol* 1985; **134**: 3798–801.
41 Visonneau S, Cesano A, Torosian MH, Miller EJ, Santoli D. Growth characteristics and metastatic properties of human breast cancer xenografts in immunodeficient mice. *Am J Pathol* 1998; **152**: 1299–311.
42 Cavacini LA, Giles-Komar J, Kennel M, Quinn A. Effect of immunosuppressive therapy on cytolytic activity of immunodeficient mice: implications for xenogeneic transplantation. *Cell Immunol* 1992; **144**: 296–310.
43 Hochman PS, Cudkowicz G, Dausset J. Decline of natural killer cell activity in sublethally irradiated mice. *J Natl Cancer Inst* 1978; **61**: 265–8.
44 Huang YW, Richardson JA, Tong AW, Zhang BQ, Stone MJ, Vitetta ES. Disseminated growth of a human multiple myeloma cell line in mice with severe combined immunodeficiency disease. *Cancer Res* 1993; **53**: 1392–6.
45 Lapidot T, Sirard C, Vormoor J *et al.* A cell initiating human acute myeloid leukaemia after transplantation into SCID mice. *Nature* 1994; **367**: 645–8.
46 Taghian A, Budach W, Zietman A, Freeman J, Gioioso D, Suit HD. Quantitative comparison between the transplantability of human and murine tumors into the brain of NCr/Sed-nu/nu nude and severe combined immunodeficient mice. *Cancer Res* 1993; **53**: 5018–21.
47 Tanaka T, Tsudo M, Karasuyama H *et al.* Novel monoclonal antibody against murine IL-2 receptor beta-chain: Characterization of receptor expression in normal lymphoid cells and EL-4 cells. *J Immunol* 1991; **147**: 2222–8.
48 Noguchi M, Yi H, Rosenblatt HM *et al.* Interleukin-2 receptor gamma chain mutation results in X-linked severe combined immunodeficiency in humans. *Cell* 1993; **73**: 147–57.
49 Puck JM, Deschenes SM, Porter JC *et al.* The interleukin-2 receptor gamma chain maps to Xq13.1 and is mutated in X-linked severe combined immunodeficiency, SCIDX1. *Hum Mol Genet* 1993; **2**: 1099–104.
50 Welsh RM. Regulation of virus infections by natural killer cells: a review. *Nat Immun Cell Growth Regul* 1986; **5**: 169–99.
51 Whiteside TL, Herberman RB. Role of human natural killer cells in health and disease. *Clin Diagn Laboratory Immunol* 1994; **1**: 125–33.
52 Whiteside TL, Vujanovic NL, Herberman RB. Natural killer cells and tumor therapy. *Curr Top Microbiol Immunol* 1998; **230**: 221–44.
53 Trapani JA, Davis J, Sutton VR, Smyth MJ. Proapoptotic functions of cytotoxic lymphocyte granule constituents *in vitro* and *in vivo*. *Curr Opin Immunol* 2000; **12**: 323–9.

Clonal analysis of thymus-repopulating cells presents direct evidence for self-renewal division of human hematopoietic stem cells

Takashi Yahata, Shizu Yumino, Yin Seng, Hiroko Miyatake, Tomoko Uno, Yukari Muguruma, Mamoru Ito, Hiroyuki Miyoshi, Shunichi Kato, Tomomitsu Hotta, and Kiyoshi Ando

To elucidate the in vivo kinetics of human hematopoietic stem cells (HSCs), $CD34^+CD38^-$ cells were infected with lentivirus vector and transplanted into immunodeficient mice. We analyzed the multilineage differentiation and self-renewal abilities of individual thymus-repopulating clones in primary recipients, and their descending clones in paired secondary recipients, by tracing lentivirus gene integration sites in each lymphomyeloid progeny using a linear amplification-mediated polymerase chain reaction (PCR) strategy. Our clonal analysis revealed that a single human thymus-repopulating cell had the ability to produce lymphoid and myeloid lineage cells in the primary recipient and each secondary recipient, indicating that individual human HSCs expand clonally by self-renewal division. Furthermore, we found that the proportion of HSC clones present in the $CD34^+$ cell population decreased as HSCs replicated during extensive repopulation and also as the differentiation capacity of the HSC clones became limited. This indicates the restriction of the ability of individual HSCs despite the expansion of total HSC population. We also demonstrated that the extensive self-renewal potential was confined in the relatively small proportion of HSC clones. We conclude that our clonal tracking studies clearly demonstrated that heterogeneity in the self-renewal capacity of HSC clones underlies the differences in clonal longevity in the $CD34^+$ stem cell pool. (Blood. 2006;108:2446-2454)

Introduction

Self-renewal and multilineage differentiation are the 2 fundamental abilities that define hematopoietic stem cells (HSCs) and distinguish them from progenitors. Severe combined immunodeficient mouse (SCID)–repopulating cells (SRCs), originally identified by their ability to reconstitute hematopoiesis in nonobese diabetic (NOD)/SCID mice, are thought to represent human HSCs that are useful clinically to repopulate human recipients.[1-3] Unlike murine HSCs that have been purified and analyzed at the single-cell level,[4] viral gene-marking is the only strategy for the in vivo clonal analysis of human HSCs.[5] Using this approach, several studies documented heterogeneity among SRC clones and implied that some clones have the ability to differentiate into B-lymphoid and myeloid lineages and to self-renew.[6-12] A major shortcoming of using the NOD/SCID mouse model is a lack of reproducible human T lymphocyte repopulation. Consequently, the multilineage differentiation capacity of SRCs in NOD/SCID recipients has been assessed by reconstitution of only B-lymphoid and myeloid lineages. Because a close relationship between B-lymphocyte and macrophage differentiation has been indicated,[13,14] current analyses cannot clearly distinguish true HSCs from lineage-restricted progenitors such as B-lymphocyte/macrophage progenitors. As a result, the multilineage differentiation and self-renewal of HSCs represented by a single SRC are yet to be proven.

Along with other investigators, we demonstrated that phenotypically normal and polyclonal human T lymphocytes were reproducibly repopulated from human cord blood $CD34^+$ cells in the NOD/SCID/common γ chain (cγ)–null (NOG) mouse.[15-17] Having this unique environment that permits human thymopoiesis, the NOG recipient serves as an excellent model to study self-renewal, as well as multilineage differentiation, of human HSCs. HSCs can be identified as thymus-repopulating cells and distinguished from short-lived oligopotent or monopotent progenitors. Thymopoiesis requires constant recruitment of progenitors into the thymus, which eventually produces mature T lymphocytes in a relatively short period of time.[18,19] Therefore, to maintain thymopoiesis in recipient mice, transplanted HSCs must divide without loss of thymus-repopulating activity. Several classes of SRCs that differ in their proliferative and self-renewal potential have been reported.[20-22]

From the Division of Hematopoiesis, Research Center for Regenerative Medicine, Tokai University School of Medicine, Isehara, Kanagawa; the Department of Hematology, Tokai University School of Medicine, Isehara, Kanagawa; the Central Institute for Experimental Animals, Kawasaki, Kanagawa; the BioResource Center, RIKEN Tsukuba Institute, Tsukuba, Ibaraki; and the Department of Cell Transplantation & Regenerative Medicine, Tokai University School of Medicine, Isehara, Kanagawa, Japan

Submitted February 8, 2006; accepted May 20, 2006. Prepublished online as *Blood* First Edition Paper, June 6, 2006; DOI 10.1182/blood-2006-02-002204.

Supported by a Grant-in-Aid for Research of the Science Frontier Program and a Grant-in-Aid for Scientific Research from the Ministry of Education, Culture, Sports, Science, and Technology of Japan and by a Research Grant on Human Genome Tissue Engineering (H17-014) from the Japanese Ministry of Health, Labor, and Welfare, Japan.

T.Y. designed and performed the research, analyzed the data, and wrote the paper; S.Y., Y.S., H. Miyatake, and T.U. performed the research; Y.M. analyzed the data and wrote the paper; M.I., H. Miyoshi, and S.K. provided vital reagents; T.H. analyzed the data; K.A. designed the research, analyzed the data, and wrote the paper.

The online version of this article contains a data supplement.

Reprints: Kiyoshi Ando, Department of Hematology, Tokai University School of Medicine, Bohseidai, Isehara, Kanagawa 259-1193, Japan; e-mail: andok@keyaki.cc.u-tokai.ac.jp.

The publication costs of this article were defrayed in part by page charge payment. Therefore, and solely to indicate this fact, this article is hereby marked "advertisement" in accordance with 18 U.S.C. section 1734.

Analyzing the thymus-repopulating activity of these cells provides a unique way to distinguish and identify long-term self-renewing stem cells within the SRCs. Self-renewal of HSCs has been assessed by serial transplantation on the basis that HSCs, which are responsible for multilineage hematopoiesis in primary recipients, are also capable of repeating this process in secondary transplant recipients. Confirmation of the persistence of thymus-repopulating cells with multilineage differentiation ability in the secondary recipient would eliminate the possible contribution of some long-lived progenitors and mature cells and at the same time, provide direct evidence for self-renewal of SRCs.

In this study, we established a novel strategy to analyze both self-renewal and multilineage differentiation of a single human thymus-repopulating SRC clone in NOG recipient mice using linear amplification-mediated polymerase chain reaction (LAM-PCR) that verifies individual genomic virus integration sites by direct sequencing.[23] The identification of specific clones in fluorescent-activated cell sorter (FACS)–sorted lymphomyeloid lineage populations by their unique molecular markers allowed us to assess how individual clones contribute to the specific lineages during long-term hematopoiesis in vivo. We focused on CD4/CD8 double-positive (DP) immature thymocyte populations as a starting point of our clonal analysis of the human HSC ability. Our study presented direct clonal evidence that a single human HSC had the ability to produce lymphoid and myeloid lineage cells. Self-renewal division of multilineage clones resulted in expansion of SRCs. However, this clonal expansion of SRCs leads to the clonal exhaustion of SRCs during long-term hematopoiesis in vivo. It was also indicated that, although most of the SRC clones were destined to loose their self-renewal potential, the relatively small proportion of SRC clones retained extensive self-renewal potential.

Materials and methods

Collection and purification of human CB CD34$^+$CD38$^-$ cells

CB samples were obtained from full-term deliveries according to the institutional guidelines approved by the Tokai University Committee on Clinical Investigation. Mononuclear cells (MNCs) were isolated by Ficoll-Hypaque (Lymphoprep, 1.077 ± 0.001 g/mL; Nycomed, Oslo, Norway) density gradient centrifugation. CD34$^+$ cell fractions were prepared using the CD34 Progenitor Cell Isolation Kit (Miltenyi Biotec, Sunnyvale, CA) according to the manufacturer's directions. Column-enriched CD34$^+$ cells were cryopreserved in liquid nitrogen until use. For isolation of CD34$^+$CD38$^-$ cells, pooled CD34$^+$-enriched cells from multiple donors were stained with fluorescein isothiocyanate–conjugated anti-CD34 (581, Coulter/Immunotech, Marseille Cedex, France), and phycoerythrin (PE)–conjugated anti-CD38 (HB7; BD Biosciences, San Jose, CA) monoclonal antibodies (mAbs). Cells were sorted using the FACSVantage flow cytometer (BD Biosciences) equipped with HeNe and argon lasers. CD38$^-$ gate was determined in reference to isotype control. CD34$^+$CD38$^-$ cells, which comprise 5% to 8% of the total CD34$^+$ cell population, were isolated with 97% to 99% (n = 16) purity using FACSVantage (BD Biosciences).

Lentivirus infection

Purified CD34$^+$CD38$^-$ cells were plated on fibronectin (FUJIREBIO, Tokyo, Japan) and incubated with highly concentrated viral supernatant at a multiplicity of infection (MOI) of 50 in serum-free StemPro-34 medium (Invitrogen, Carlsbad, CA) containing cytokines (Takara Shuzo, Tokyo, Japan) for 16 hours. Recombinant human thrombopoietin (50 ng/mL; kindly donated by Kirin Brewery, Tokyo, Japan), stem cell factor (50 ng/mL; donated by Kirin Brewery, Tokyo, Japan), and Flk-2/Flt-3 ligand (50 ng/mL; R&D Systems, Minneapolis, MN) were used. The number of virus integration sites per cell was examined in the following experiment. CD34$^+$ cells were infected with enhanced green fluorescent protein (EGFP) at an MOI of 50 and then plated in methylcellulose. Individual colonies expressing EGFP were picked up and analyzed for integration sites by LAM-PCR. Over the 20 colonies examined, none of the colonies demonstrated multiple bands, confirming that the individual colonies contain a single integration site (data not shown).

Estimation of multilineage differentiation potential of SRCs

NOD/Shi-scid, IL-2Rγc^{null} (NOG) mice were obtained from the Central Institute for Experimental Animals (Kawasaki, Japan) and maintained in the animal facility of the Tokai University School of Medicine in microisolator cages; the animals were fed with autoclaved food and water. Nine- to 20-week-old NOG mice were irradiated with 250 cGy X-rays. The following day, transduced CD34$^+$CD38$^-$ cells (1×10^4 cells) were injected intravenously into the NOG mice. All experiments were approved by the animal care committee of Tokai University. Sixteen to 20 weeks after transplantation, the mice were humanly killed, and bone marrow (BM) cells, splenocytes, and thymocytes were analyzed by flow cytometry. Cells were stained with mAbs to human leukocyte differentiation antigens. Human hematopoietic cells were distinguished from mouse cells by the expression of human CD45. APC-conjugated anti–human CD19 mAb (Coulter/Immunotech), ECD-conjugated anti–human CD8 and CD34 mAbs (all Coulter/Immunotech), and PE-conjugated anti–human CD3, CD4, and CD33 mAbs were used. The efficiency of gene transduction was determined by the percentage of cells expressing EGFP. EGFP-expressing CD45$^+$ human hematopoietic cells were further classified into human stem/progenitor (CD34$^+$), myeloid (CD33$^+$), B-lymphoid (CD19$^+$), and T-lymphoid (CD3$^+$ or CD4$^+$/CD8$^+$) subpopulations and were sorted using a FACSVantage Diva option (BD Biosciences). To eliminate the contamination of lineage-committed cells, CD34$^+$ cells were sorted on CD19$^-$ and CD33$^-$ gate. Sorted cells, confirmed to be lineage^{low}CD34$^+$, were designated as stem/progenitor cells. Double cell-sorting was performed to ensure greater than 99% cell purity. Representative FACS profiles of sorting purity were demonstrated in Figure S1 (available at the *Blood* website; see the Supplemental Materials link at the top of the online article).

Secondary transplantation

BM cells were obtained from mice that received a transplant with CD34$^+$CD38$^-$ cells at 13 to 19 weeks after transplantation. The BM cells of these primary recipients were divided equally and injected intravenously into 2 sublethally irradiated secondary NOG recipients (1.35×10^7–2.1×10^7 cells per recipient). Thirteen to 19 weeks after transplantation, BM cells and thymus were collected from each secondary recipient and used for flow cytometric analysis and lineage cell sorting as described.

Integration site analysis of lentivirally marked SRCs

LAM-PCR was carried out as described previously[24] with some slight modifications. Genomic DNA samples (100 ng), isolated from each sorted subpopulation, were preamplified for a total of 100 cycles by repeated primer extension using 0.25 pmol vector-specific, 5′-biotinylated primer LTR1 (5′-GAACCCACTGCTTAAGCCTCA-3′) using ProofStart DNA polymerase (2.5 U; Qiagen, Hilden, Germany). The biotinylated extension products were collected using streptavidin-conjugated magnetic beads (Dynal, Oslo, Norway), and the second strand was synthesized using Klenow polymerase (2 U; Takara Shuzo) and random primer (Takara Shuzo). To prevent virus-vector sequence contamination, samples were first incubated with SacI endonuclease (5 U; Promega, Madison, WI) for 2 hours at 37°C and then digested with Esp3I endonuclease (5 U; New England BioLabs, Ipswich, MA) for 2 hours at 65°C. After restriction digestion, 100 pmol of a linker cassette (5′-GTAGATAATGGTCGTAGACAGCGTAAT-ACGACTCACTATAGGGAGA-3′) were ligated using a DNA ligation kit (Takara Shuzo) at 16°C overnight. Each ligated sample was amplified using a vector-specific primer, LTR2 (5′-AGCTTGCCTTGAGTGCTTCA-3′)

and a linker cassette primer (5′-GTAGATATTGTCGTTAGAACGCGTA-ATACGACTCA-3′), using the following conditions: 95°C for 1 minute, 60°C for 1 minute, 72°C for 1 minute (30 cycles). Each PCR product was subjected to nested PCR with the internal primers, LTR3 (5′-AGTAGTGTGTGCCCGTCTGT-3′) and LC2 (5′-CGTTAGAACGCGTA-ATACGACTCACTATAGGGAGA-3′), under identical conditions. PCR products were sequenced after cloning into the TOPO TA cloning vector (Invitrogen). The proviral integration sites of DP cells were sequenced, and the sequences were examined for alignment to the human genome using NCBI BlastN (http://www.ncbi.nlm.nih.gov/blast). The verified genomic sequence information of these DP cell integration sites was used to design new primers (all primer sequences used in this study are listed in Tables S1-S3). PCR was performed on each LAM-PCR product using the unique genomic flanking primers in combination with the LTR3 primers.

Estimation of clone size by real-time quantitative PCR (RQ-PCR)

Genomic DNA samples from CD34$^+$ cells of secondary recipients were amplified using multiple displacement amplification reagents (REPLI-g; Qiagen) according to the manufacturer's instructions.[25] Briefly, 10 ng template DNA was mixed with the DNA polymerase and incubated for 16 hours at 30°C. Approximately 50 μg amplified DNA was obtained from each sample. For RQ-PCR, each target DNA was amplified on the same plate with β-globin as the reference using the QuantiTect SYBR Green PCR Master Mix (Qiagen) and the ABI Prism 7700 Sequence Detection System (Applied Biosystems). The relative clone amounts and range were determined in reference to β-globin. Threshold cycles (C_T) were determined as to fit all samples in logarithmic phase. To ensure the efficiency of amplification and the assay precision, calibration curves for each clone sequence were constructed to have the correlations (r^2) of above 0.95 and the efficiency of greater than 98%. A comparative C_T was used to determine the proportion of CD34$^+$ clones in paired secondary recipients that were derived from the parent primary recipient clone. For each sample, the clone C_T value was normalized using the formula ΔC_T = ΔC_T clone − ΔC_T β-globin. To determine relative clone size, the following formula was used: $\Delta\Delta C_T$ = ΔC_T clone in CD34+ cells of the one secondary recipient − ΔC_T clone in CD34+ cells of the other secondary recipient, and the value was calculated by the expression $2^{-\Delta\Delta C_T}$. Each reaction was performed at least in triplicate. Amplification conditions were as follows: 95°C for 15 minutes followed by 40 cycles at 95°C for 15 seconds, 60°C for 30 seconds, and 72°C for 60 seconds.

The same primer set described in PCR tracking of LAM-PCR procedure was used to amplify each clone. As an internal control, human hematopoietic cell kinase 1 (*HCK1*) gene and ribosomal DNA (*rDNA*) gene were also amplified. Even amplification of each genomic DNA was confirmed by RQ-PCR using all 3 internal control primers (data not shown).[26] The primers for β-globin gene were forward, 5′-GTGCACCTGACTCCTGAG-GAGA-3′, and reverse, 5′-CCTTGATACCAACCTGCCCAG-3′. Primers for *HCK1* gene were forward, 5′-TATTAGCACCATCCATAGGAGGCTT-3′, and reverse, 5′-GTTAGGGAAAGTGGAGCGGAAG-3′. Primers for *rDNA* gene were forward, 5′-CCATCGAACGTCTGCCCTA-3′, and reverse, 5′-TCACCCGTCGTCACCATG-3′.

Statistical analysis

Data are represented as mean ± SD. The 2-sided *P* value was determined by testing the null hypothesis that the 2 population medians are equal. *P* values less than .05 were considered to be significant.

Results

Multilineage differentiation of gene-marked SRCs

To investigate the multilineage differentiation and self-renewal capacity of individual SRC clones, we introduced recombinant lentiviral vector carrying an EGFP-encoding gene to cord blood CD34$^+$CD38$^-$ cells which can provide long-term engraftment (more than 12 weeks) and multilineage differentiation,[2] and then we transplanted these cells into sublethally irradiated NOG mice. Multilineage differentiation was determined as the proportion of each hematopoietic lineage within the EGFP-expressing human CD45$^+$ cell population using FACS at 16 to 20 weeks after transplantation (Figure 1). Consistent with our previous results,[16] substantial engraftment, including CD34$^+$ primitive cells, CD33$^+$ myeloid, CD19$^+$ B-lymphoid, CD3$^+$ mature, and DP immature T-lymphoid cells, was observed in the BM, spleen, and thymus of the NOG mice (Table 1). Because the proportion of nontransduced EGFP$^-$ cells within the human graft and the percentage of EGFP$^+$ cells within each lineage were not significantly different (data not shown), these data indicated that EGFP transduction did not affect the differentiation and proliferation capacity of the SRCs.

Multilineage differentiation of individual thymus-repopulating SRC clones

To analyze the multilineage differentiation capacity of individually transduced SRCs, we performed in vivo integration site analysis by LAM-PCR that can distinguish the progeny of each transduced cell

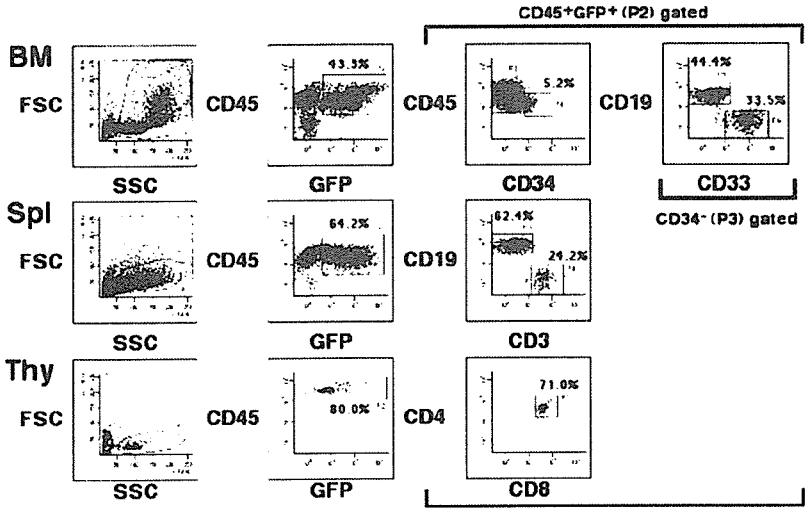

Figure 1. Representative FACS profiles of EGFP-transduced SRCs. Samples were obtained from BM, spleen, and thymus of a NOG mouse, and the proportion of EGFP-transduced human cells was evaluated. The relative frequencies of each cell population are indicated.

Table 1. Proportion of each human cell lineage engrafted in primary NOG mice

Mouse	Week*	Bone marrow, % engrafted					Spleen, % engrafted				Thymus, % engrafted		
		CD45	EGFP	S	M	B	CD45	EGFP	T	B	CD45	EGFP	T
1	17	82.2	84.8	22.1	4.6	ND	81.8	65.3	2.1	88.6	97.8	83.0	82.6
3	17	74.0	58.5	5.2	33.5	44.4	82.1	78.2	24.2	62.4	85.5	80.0	71.0
4	16	88.9	75.4	8.5	17.5	64.4	75.6	77.9	1.6	87.9	95.0	52.9	23.4

The total cellularity of BM and thymus in the primary recipient was $3.56 \times 10^7 \pm 0.53 \times 10^7$ and $1.39 \times 10^8 \pm 1.13 \times 10^8$, respectively. Each mouse listed in the table received a transplant of 10×10^3 CD34$^+$ CD38$^-$ cells.

S indicates CD34$^+$ stem/progenitor cells; M, CD33$^+$ myeloid lineage cells; B, CD19$^+$ B lymphoid lineage cells; T, CD3$^+$ (spleen) or CD4/CD8 double-positive (thymus) T lymphoid lineage cells; ND, not done.

*Weeks after transplantation. Bone marrow cells, spleen cells, and thymocytes of NOG mice were stained with an anti-human CD45 mAb and analyzed. The proportion of EGFP-expressing cells within the CD45$^+$ cells and cells positive for each lineage marker in the CD45$^+$/EGFP$^+$ was calculated.

by its unique proviral-genomic fusion sequence (Figure 2A). Direct sequencing of PCR products derived from EGFP$^+$ CD45$^+$ DP cells verified that each product with a unique band length represented individual and different clones. LAM-PCR analysis of EGFP$^+$ CD45$^+$ FACS-purified lineage populations detected multiple integration sites in each cell lineage (Figure 2B). It is reported that the number of vector copies per cell can be controlled by adjusting the MOI, without reducing the transgene expression levels.[27] Because we optimized the experimental conditions to have each cell carrying one insertion per cell, confirmed by both colony-forming assay (see "Materials and methods") and transplantation assay,[24] multiple integration sites detected by LAM-PCR indicated polyclonal repopulation in the NOG mice.

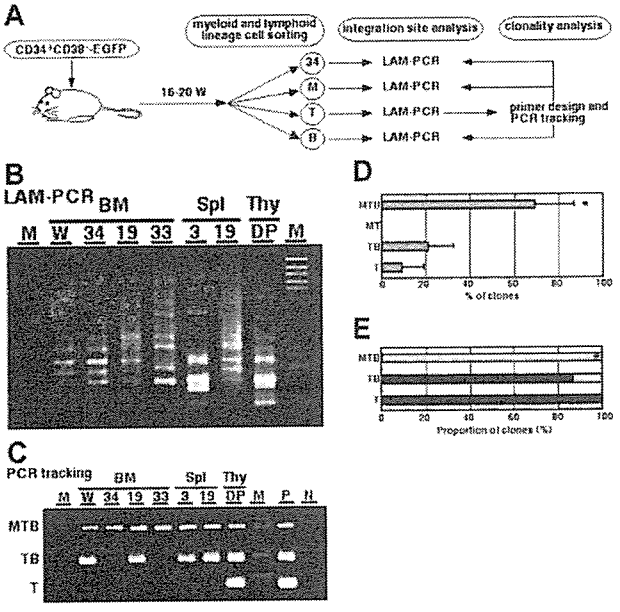

Figure 2. Clonal analysis of primary transplanted SRCs. (A) Study design for clonal analysis of primary grafts. 34 indicates CD34$^+$ stem/progenitor cells; M, CD33$^+$ myeloid lineage cells; B, CD19$^+$ B lymphoid lineage cells; T, CD3$^+$ (spleen) or CD4/CD8 double-positive (thymus) T lymphoid lineage cells. (B) Representative LAM-PCR profiles of SRCs. Each band represents a different insertion locus in the assayed material. W indicates unseparated whole BM MNCs; M, size marker. (C) DP-derived T lymphoid insertion sites were traced by PCR. The clones detected in all lymphomyeloid lineage cells were designated as multipotent type (MTB). TB indicates clones restricted in T lymphoid and B lymphoid cells. T clones detected in T lymphoid cells; W, unseparated whole BM MNCs; M, size marker; P, IA-cloned LAM-PCR product was used as a positive control; N, DW. (D) Relative frequencies of each clone type detected in primary SRCs. Data represent mean ± SD of 3 independent experiments. $^*P < .01$ relative to other type of clones. (E) Proportion of clones detected in the CD34$^+$ cell population. A total of 27 clones in 3 independent experiments were analyzed. Gray bars represent the clones detected in CD34$^+$ cells. Black bars represent the clones not detected in DP cells. $^*P < .01$ relative to other type of clones.

A total of 27 clones were identified in 3 independent experiments based on the genomic sequence information of the LAM-PCR products from the DP cells (Table S1 summarizes the results of the integration site analysis of DP cells). Using primers designed to correspond to individual integration sites, and therefore unique clones, we were able to track the individual clones and their progenies, including CD34$^+$ stem/progenitor, myeloid, and B-lymphoid cells (Figure 2A). Three different clone types were observed in this experiment (Figure 2C): a multipotent type (MTB), in which insertion sites originally detected in the DP cells were also detected in the highly purified myeloid and B-lymphoid cell populations; a unipotent progenitor containing exclusively T cells; and a bipotent T/B progenitor. However, a bipotent progenitor containing myeloid and T lymphocytes was not detected. As expected, analysis of thymus-repopulating cells revealed that the majority of SRC clones (70.4%) found in the recipient mice were of the MTB multilineage type (Figure 2D; Table 2). We also used CD14 and CD66b, a more mature myeloid marker, for clonal analysis and detected the equivalent proportion of the 3 clone types (data not shown). Interestingly, all MTB clones were found in the CD34$^+$ cell population (Figure 2E), suggesting that the transduced SRC clones self-replicated within the CD34$^+$ stem cell pool without losing their ability to contribute to both lymphoid and myeloid lineages during long-term hematopoiesis. However, as the differentiation capacity of clones became limited to bipotency or unipotency, the proportion of clones that were also found in the CD34$^+$ cell population decreased (Figure 2E), indicating that some SRC clones had been exhausted from the stem cell pool during lineage commitment.

In vivo expansion of individual thymus-repopulating SRC clones

To directly demonstrate the self-renewal capacity of the SRCs, we injected BM cells from each primary mouse into 2 secondary mice

Table 2. Differentiation potential of thymus-repopulating SRC clones

Mouse	No. of clones	Clone type, no. (%)		
		MTB	TB	T
1	5	3 (60)	1 (20)	1 (20)
3	12	7 (58.3)	4 (33.3)	1 (8.3)
4	10	9 (90)	1 (10)	0 (0)
Total	27	19 (70.4)	6 (22.2)	2 (7.4)

Extensive contribution of individual thymus-repopulating SRC clones was evaluated by LAM-PCR tracking based on integration site analysis of DP cells. No clones were differentiated into M and T lineages.

MTB indicates clones that gave rise to myeloid (M), T lymphoid (T), and B lymphoid (B) lineages. TB, clones differentiated into T and B lineages. T, clones differentiated into T lineage only.

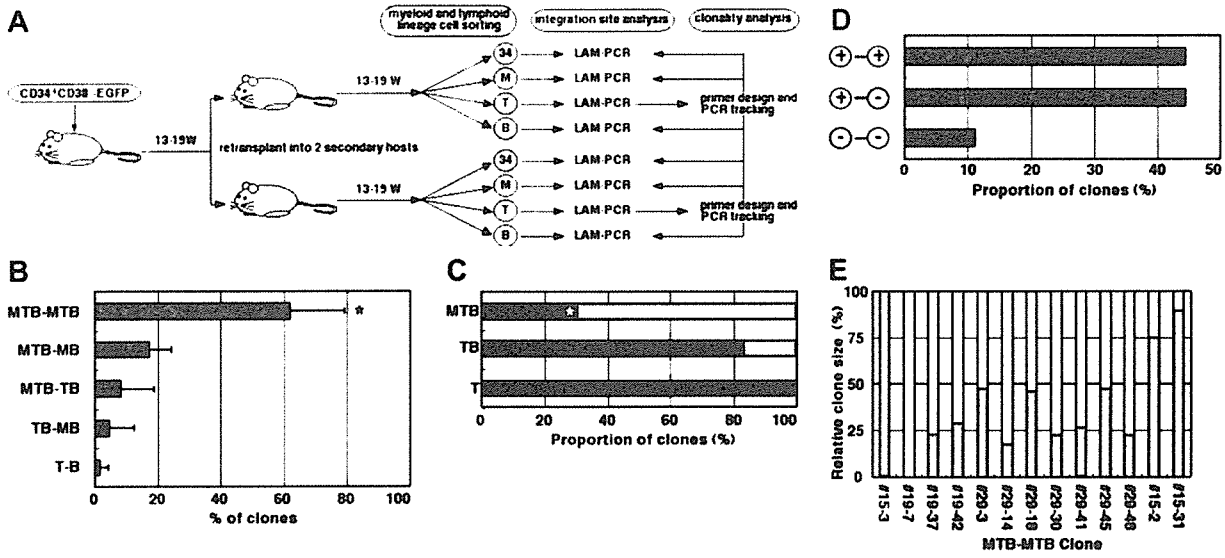

Figure 3. Clonal analysis of secondary transplanted SRCs. (A) Study design for clonal analysis of secondary grafts. 34 indicates CD34+ stem/progenitor cells; M, CD33+ myeloid lineage cells; B, CD19+ B-lymphoid lineage cells; T, CD3+ (spleen) or CD4/CD8 double-positive (thymus) T lymphoid lineage cells. (B) Relative frequencies of each clone type detected in paired secondary transplanted recipients. Data represent mean ± SD of 3 independent experiments. *P < .01 relative to other type of clones. (C) The proportion of clones detected in CD34+ cells is shown. A total of 43 clones in 3 independent experiments were analyzed. Gray bars represent the clones detected in CD34+ cells. Black bars represent the clones not detected in CD34+ cells. *P < .01 relative to MTB clones found in primary recipients (shown in Figure 1E). (D) The proportion of MTB clones found in CD34+ cells of paired secondary recipients. A total of 27 clones in 3 independent experiments were analyzed. Notation of the left vertical axis: +/+, MTB-MTB clone pairs were detected in CD34+ cells of both secondary recipient pairs; +/-, MTB-MTB clone pairs were detected in the CD34+ cells of 1 of the 2 secondary recipient pairs; and -/-, MTB-MTB clone pairs were not detected in the CD34+ cells of either secondary recipient pairs. (E) Relative clone size of individual clones in each MTB-MTB clone pairs in CD34+ stem cell pool found in paired secondary recipient. The relative clone size of individual clones in 11 MTB-MTB clone pairs detected in CD34+ cells of both secondary recipients was examined by RQ-PCR. The relative clone size of individual clones in each MTB-MTB pair is expressed as the proportion of one clone relative to the other clone. The MTB-MTB clone pairs no.15-3 and no. 19-7 that was detected in the CD34+ cells of only 1 of the 2 secondary recipient pairs were used as experimental control and demonstrated complete skewing to either one recipient.

(Figure 3A). Although each primary BM cell population was divided into 2 recipients, substantial engraftment was observed in these secondary-recipient NOG mice (Table 3). Clone tracking analysis was then performed to examine the fate of individual SRC clones in paired secondary mice. Integration site analysis by LAM-PCR of FACS-sorted cells showed polyclonal reconstitution in each secondary host. A total of 43 clones were identified by integration site analysis of DP T lymphocytes found in 3 secondary recipient pairs (results are summarized in Table S2). All clones detected in paired secondary recipients were also detected in the primary donor. Strikingly, all 43 clones were found as a pair: clones detected in one of the secondary recipient pairs were always observed in the other pair. In greater than 90% of these clone pairs (39 of 43), at least 1 of the daughter clones inherited MTB differentiation potential from its parent clone. Moreover, in 69.2% of these 39 clone pairs, both daughter clones remained multipotent (MTB-MTB type), whereas the other daughter clone in the remaining 30.8% of clone pairs became committed to specific cell lineages (MTB-MB or MTB-TB type) (Figure 3B; Table 4). The existence of MTB-MTB type clones in secondary recipients indicated that a single SRC clone self-replicated in the primary recipients and produced 2 daughter clones that retained SRC potential, thereby resulting in the in vivo expansion of multipotent SRC clones.

Table 3. Proportion of the primary and the secondary human graft

Mouse	Cell dose*	Week†	Bone marrow, %					Thymus, %		
			CD45	EGFP	S	M	B	CD45	EGFP	T
Primary recipient										
101	17	13	80.3	72.7	ND	ND	ND	ND	ND	ND
109	6	19	66.2	71.0	ND	ND	ND	ND	ND	ND
113	10	14	43.2	71.8	ND	ND	ND	ND	ND	ND
Secondary recipient										
101-1	21	13	63.0	93.3	3.4	7.4	63.7	98.2	80.1	83.6
101-2	21	13	62.5	88.1	4.2	14.6	54.9	96.5	78.6	71.2
109-1	13.5	17	29.4	69.4	1.3	49.5	29.9	91.3	78.2	90.5
109-2	13.5	17	33.3	75.1	1.9	27.6	45.9	93.0	70.1	81.1
113-1	19.3	19	72.3	68.7	3.4	17.3	38.7	95.5	88.1	88.0
113-2	19.3	19	86.3	50.0	0.6	17.2	17.3	92.9	72.3	70.3

The total cellularity of BM in the primary and the secondary recipient was 3.86×10^7, 0.83×10^7 and 3.72×10^7, 0.91×10^7, respectively. The total cellularity of thymus in the primary and the secondary recipient was 3.36×10^8, 3.28×10^7 and 2.43×10^8, 1.59×10^7, respectively.

ND indicates not done.

*Number of CD34+CD38- cells transplanted (primary recipient, 10^5; secondary recipient, 10^4).

†Number of weeks after transplantation.

Table 4. Differentiation potential of paired secondary clones

Mouse	No. of clones	Clone type, no. (%)				
		MTB-MTB	MTB-MB	MTB-TB	MB-TB	T-B
101	22	12 (54.5)	5 (22.7)	1 (4.5)	3 (13.6)	1 (4.4)
109	11	9 (81.8)	2 (18.2)	0 (0)	0 (0)	0 (0)
113	10	6 (60)	2 (20)	2 (20)	0 (0)	0 (0)
Total	43	27 (62.8)	9 (20.9)	3 (7)	3 (7)	1 (2.3)

Differentiation potential of paired secondary clones was determined by PCR tracking strategy based on integration site analysis of DP cells developed in secondary recipients.

Individual thymus-repopulating SRC clones have different self-renewal capacities

Consistent with our earlier observations in the primary recipient mice, the proportion of MTB clones present in the $CD34^+$ cell population decreased as the differentiation capacity of the clones became limited (Figure 3C). In addition, note that 30.3% of MTB clones in the secondary recipient mice were no longer found in the $CD34^+$ cell population, contrasting with the initial finding that all MTB clones in the primary mice were found in the $CD34^+$ cell population (Figure 2E). Therefore, phenotypic and possibly functional differences exist between MTB clones in the primary and secondary recipient mice, although both were capable of repopulating and giving rise to multilineage progenitors in the host. To assess how the MTB clone cell division affected the status of daughter MTB clones, we examined how many of in vivo–expanded MTB-MTB clone pairs were also found in the $CD34^+$ cell population and classified into 3 groups (Figure 3D). First, in 44.4% of the MTB-MTB clone pairs, both daughter clones were found in the $CD34^+$ cell population. Second, in another 44.4% of MTB-MTB clone pairs, only one of the daughter clones was found in the $CD34^+$ cell population. These results indicated that the former type clones have relatively higher SRC activity and that, as a result of unequal distribution of SRC activity in 2 daughter clones after cell division, 1 of the daughter clones exited from the $CD34^+$ stem cell pool. Finally, in 11.1% of MTB-MTB clone pairs, neither daughter clone was detected in the $CD34^+$ stem cell pool, which may reflect the extensive replication required to repopulate both primary and secondary recipients that eventually leads to exhaustion of the stem cells. These results demonstrate the heterogeneity among clones that repopulate both the primary and secondary recipient mice.

To further confirm our findings of heterogeneity of SRC clones, we quantitatively examined what was the relative clone size ratio of each MTB-MTB clone pair in the $CD34^+$ stem cell pool by RQ-PCR. In the majority of MTB-MTB clone pairs, the proportion of individual clone in each clone pair varied widely (Figure 3E). Interestingly, only a small proportion of MTB-MTB clone pairs (no. 29-3, no. 29-18, and no. 29-45) were found to be equally distributed to each paired recipient. Those clone pairs that were able to repopulate equally in a paired secondary recipient may have more extensive self-renewal capacity. The results indicated that individual thymus-repopulating SRC clones have different self-renewal capacities, which is a basis for a hierarchically organized stem cell pool.

We also performed tertiary transplantation and analyzed SRC clones found in the recipients. The level of engraftment in tertiary recipients was less than 1% in BM and 0.1% in the thymus ($n = 4$). We performed integration site analysis on unseparated BM MNCs of tertiary recipients and obtained 17 clones from 4 mice. The status of individual tertiary SRC clones in the secondary recipients was examined by clone tracking analysis using the LAM PCR products from tertiary graft as a starting point of clonal analysis. We found that all SRC clones in the tertiary mice were detected in the $CD34^+$ stem cell pool of secondary recipient (Table S3 summarizes the results of the integration site analysis of SRCs). The results of tertiary transplantation experiment confirmed that only HSC clones that continuously replicate themselves in the $CD34^+$ stem cell pool could produce descendents to maintain long-term hematopoiesis.

Discussion

This study provides the first direct evidence for the multilineage differentiation and self-renewal of human HSCs at the single-cell level in vivo using PCR tracing analysis of individual thymus-repopulating clones. We demonstrated that polyclonal thymus-repopulating clones with multilineage differentiation and self-renewal abilities were able to maintain long-term human hematopoiesis. This study revealed several features of human HSCs that are important biologically and clinically. First, self-renewal division of individual thymus-repopulating clones resulted in clonal expansion of cells with multilineage differentiation in vivo. Second, a single thymus-repopulating clone produced progeny that were heterogeneous in SRC activity. Third, as a result of continuous division and/or advancement of lineage commitment, some of these multipotent thymus-repopulating clones were destined to limit their capability for multilineage differentiation and self-renewal. Our study indicated that, although the majority of thymus-repopulating clones loose their self-renewal potential, a relatively small proportion of thymus-repopulating clones retain extensive self-renewal potential. Therefore, the self-renewal capacity distinctly different in individual thymus-repopulating clones may cause a hierarchically organized stem cell pool.

Controlling the copy number of the virus vector in each transduced cell is important for our clonality analysis. We recently reported the direct evidence for single virus integration per cell in a transplantation study.[24] When EGFP-transduced $CD34^+$ cells expanded in vitro were divided and transplanted into multiple recipient mice, the unique integration site representing individual clones were detected in multiple mice; in other words, multiple mice were engrafted with the same clone. If a cell contains more than one integration site and assessed as "different" clones, these different clones should be detected in the same recipients. However, none of the clones demonstrated the identical engraftment pattern. In addition, clonal tracking analyses in this study clearly demonstrated that the individual SRC clones were both qualitatively and quantitatively heterogenous. Everything being considered, our infection condition achieves one copy per cell. Even if there is a slight possibility that the number of copies per cell is more than one, the clonality is not denied. Because a virus gene integrates into the host genome at a random site, progenies having a common integration site are developed from a single clone. It could affect the numeric calculation of the number of clones, but it would not influence our interpretation of the result.

Although the concept of HSCs was proposed decades ago and is well accepted, little experimental data regarding multipotency of human HSCs is available. Using a genetic marking strategy in both experimental[6-12] and clinical studies,[28-33] it has been suggested that hematopoietic reconstitution after transplantation is attributed to oligoclonal or polyclonal HSC activity and that the repopulation capacity of individual HSCs is substantially heterogeneous. However, the results of these studies, such as the presence of transgene expression in B lymphocytes and myeloid cells and the detection of similar genomic bands in multiple hematopoietic recipient organs, were not sufficient to unequivocally determine the multipotency of human HSCs at the single-cell level. Recently, Schmidt et al[34] reported clonal evidence for multilineage

human hematopoietic differentiation from IL-2Rcγ gene-transduced CD34$^+$ cells transplanted into patients with X-linked SCID. Considering that the IL-2Rcγ has been known to play a critical role in lymphoid development,[35] the observations based on the IL-2Rcγ gene-expressing clone may not reflect authentic hematopoietic development because of possible lineage commitment redirection mediated by cytokines that act on IL-2Rcγ. Although the HSC's potential was elaborately assessed clonally in vitro,[36,37] there exists some concerns; the lineage commitment could be easily fluctuated by culture conditions; homing of HSCs to thymus was neglected. The field has thus far lacked experimental evidence showing that purified human HSCs possess the potential for multilineage differentiation at the single-cell level. In this study, we succeeded in demonstrating that a single HSC gave rise to myeloid, T-, and B-lymphoid lineage cells by using LAM-PCR–based clonal tracing analysis in highly purified lymphomyeloid cell populations. Our results now provide data supporting the multipotency of a single human HSC.

Transplantation of prospectively isolated donor cells in mice has demonstrated that only HSCs can sustain thymopoiesis for a long period.[38,39] A lack of reliable in vivo experimental models for human thymocyte reconstitution and clonal stem cell assays has precluded determining whether the same applies to human HSCs. In this study, we used the thymus-repopulating potential of individual SRC clones as a means to analyze human HSCs at a single-cell level in vivo. Previously, we have demonstrated that human T lymphocytes derived from CD34$^+$ cells and developed in NOG recipient mice bore polyclonal Vβ TCR and responded not only to mitogenic stimuli but also to allogeneic human cells, which reflects normal human T-lymphoid cell development.[16-19] By analyzing individual thymus-repopulating clones in the NOG recipient, we successfully demonstrated that human thymus-repopulating cells were derived from a single multipotent-type HSC clone and were capable of maintaining long-term thymopoiesis in vivo. This is the first clonal evidence that multipotent HSCs contribute to long-term human thymopoiesis.

Self-renewal is essential for HSCs to maintain homeostasis in the blood system by the sequential generation of mature blood cells throughout a lifetime. To maintain the total pool of HSCs, this ability must be passed on to at least one of the daughter cells in each division. If both daughter cells undergo terminal differentiation, HSCs will eventually be lost. On the other hand, if both daughter cells retain stem cell properties, the total number of HSCs will increase, resulting in expansion of HSCs.[40] In fact, an increase in the number of murine[41,42] (and human[43,44]) repopulating cells was reported in serial transplantation studies. Limiting dilution analysis showed that secondary recipients contained larger numbers of HSCs than was originally injected. These results suggest that HSCs can replicate vigorously under certain conditions. However, it has been shown that HSCs intrinsically limit their potential for self-renew.[45-47] Recently, Ema et al[48] observed the self-renewal ability of HSCs by single murine HSC serial transplantation experiments and statistically determined that the number of HSCs increased in the BM of recipients, although the mean activity of individual HSCs was reduced. Taken together, this finding suggests that, although HSCs replicate themselves, which results in expansion of HSCs, they sequentially loose their potential as a HSC. Our clonal analysis of thymus-repopulating cells in paired secondary recipients provides direct evidence to address this innate property of HSCs in vivo.

Our finding that the same multipotent HSC clone was detected in paired secondary recipients (MTB-MTB type) indicates that a single SRC clone can self-replicate to produce 2 daughter cells with multilineage differentiation and self-renewal potential, leading to the in vivo expansion of SRCs. It has been considered that SRCs that can engraft and give rise to multilineage cells in secondary recipients are self-renewed HSCs. Thus, these MTB-MTB clones in this study could be defined as HSCs. However, when the MTB-MTB clone pairs were further examined whether they remained in the stem cell pool, one of the daughter clones in the pair was no longer found in the CD34$^+$ cell population in approximately half of MTB-MTB clone pairs. Furthermore, the stem cell phenotype was not retained in 11.1% of MTB-MTB clones. Considering that 100% of MTB clones in primary recipients possess the stem cell phenotype, these results indicate that SRCs with the stem cell phenotype progressively decrease during serial transplantation, leading to exhaustion of SRCs. This is consistent with our finding that the proportion of clones with the stem cell phenotype decreased as the clone committed to specific lineages. By assessing the phenotype of self-replicated multilineage clone pairs, determined by the presence of common integration site in CD34$^+$ cell population, we were able to reveal the status of HSCs during aging. The loss of stem cell phenotype may be caused by extensive replication required for hematopoietic reconstitution in recipient. Although the total SRC population appears to expand, our data indicate that the ability of individual SRCs, in more than half of the clones, may become restricted during long-term hematopoiesis in vivo.

Our clonal tracking analysis clearly demonstrated that heterogeneity in the self-renewal capacity of individual multipotent SRC clones underlies the differences of clonal longevity in the stem cell pool (Figure 4). Although most of the SRC clones loose their self-renewal potential, a relatively small proportion of SRC clones

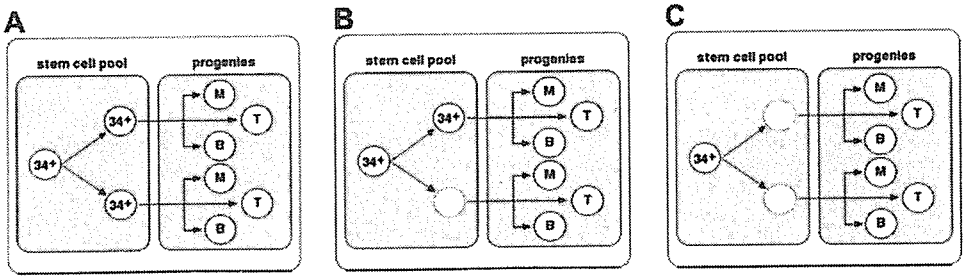

Figure 4. Schema of in vivo expansion. (A) A HSC replicates and produces 2 daughter cells, both of which retain the HSC phenotype. The paired daughter HSCs in the stem cell pool contribute to hematopoiesis; even so, the self-renewal activity of the parent HSC may be equally distributed to both daughters or may be skewed to either daughter cell. (B) As a result of heterogeneous HSC replication, one of the daughter HSCs loses the stem cell potential and therefore exits from the stem cell pool, but still remains in the progenitor pool. (C) Both paired daughter cells have lost their HSC potential, leading to exhaustion from the stem cell pool. 34 indicates CD34$^+$ stem/progenitor cells; M, CD33$^+$ myeloid lineage cells; B, CD19$^+$ B lymphoid lineage cells; T, CD3$^+$ (spleen) or CD4/CD8 double positive (thymus) T lymphoid lineage cells.

(3 of 43 total secondary descending clones) are able to continuously self-renew. Our strategy which combined lineage-cell sorting and LAM-PCR enabled identification of the MTB clone that continuously self-renews in the stem cell pool and represents the long-term HSC. Our study provides a method that can accurately evaluate in vivo properties of human HSCs, and further studies may lead to elucidation of the mechanisms of self-renewal of the long-term human HSC at the single-cell level. It has been demonstrated that long-term leukemic stem cells have extensive self-renewal potential, and their hierarchic organization of stem cell pool was notably similar to the normal HSC compartment.[49,50] These findings propose the idea that some forms of leukemia imitate a system of the normal long-term HSC and retain or acquire the extensive self-renewal capacity. The clonal analysis for properties of long-term HSCs in vivo will be a powerful tool to understand the mechanisms for tumor initiation, progression, and relapses and will lead to efficient use of HSCs in clinical transplantation medicine.

Acknowledgments

We thank Tadayuki Sato, Hideyuki Matsuzawa, and Hideo Tsukamoto of the Teaching and Research Support Center of Tokai University for technical assistance; members of the animal facility of Tokai University, especially Mayumi Nakagawa, for meticulous care of the experimental animals; and members of the Tokai Cord Blood Bank for their assistance. We also thank members of the Research Center for Regenerative Medicine of Tokai University for helpful discussion and assistance.

References

1. Larochelle A, Vormoor J, Hanenberg H, et al. Identification of primitive human hematopoietic cells capable of repopulating NOD/SCID mouse bone marrow: implications for gene therapy. Nat Med. 1996;2:1329-1337.
2. Bhatia M, Wang JC, Kapp U, Bonnet D, Dick JE. Purification of primitive human hematopoietic cells capable of repopulating immune deficient mice. Proc Natl Acad Sci U S A. 1997;94:5320-5325.
3. Wang JC, Doedens M, Dick JE. Primitive human hematopoietic cells are enriched in cord blood compared with adult bone marrow or mobilized peripheral blood as measured by the quantitative in vivo SCID-repopulating cell assay. Blood. 1997;89:3919-3924.
4. Osawa M, Hanada K, Hamada H, Nakauchi H. Long-term lymphohematopoietic reconstitution by a single CD34-low/negative hematopoietic stem cell. Science. 1996;273:242-245.
5. Lemischka IR, Jordan CT. The return of clonal marking sheds new light on human hematopoietic stem cells. Nat Immunol. 2001;2:11-12.
6. Woods NB, Fahlman C, Mikkola H, et al. Lentiviral gene transfer into primary and secondary NOD/SCID repopulating cells. Blood. 2000;96:3725-3733.
7. Guenechea G, Gan OI, Dorrell C, Dick JE. Distinct classes of human stem cells that differ in proliferative and self-renewal potential. Nat Immunol. 2001;2:75-82.
8. Ailles L, Schmidt M, Santoni de Sio FR, et al. Molecular evidence of lentiviral vector-mediated gene transfer into human self-renewing, multipotent, long-term NOD/SCID repopulating hematopoietic cells. Mol Ther. 2002;6:615-626.
9. Piacibello W, Bruno S, Sanavio F, et al. Lentiviral gene transfer and ex vivo expansion of human primitive stem cells capable of primary, secondary, and tertiary multilineage repopulation in NOD/SCID mice. Nonobese diabetic/severe combined immunodeficient. Blood. 2002;100:4391-4400.
10. Barquinero J, Segovia JC, Ramirez M, et al. Efficient transduction of human hematopoietic repopulating cells generating stable engraftment of transgene expressing cells in NOD/SCID mice. Blood. 2000;95:3085-3093.
11. Josephson NC, Vassilopoulos G, Trobridge GD, et al. Transduction of human NOD/SCID repopulating cells with both lymphoid and myeloid potential by foamy virus vectors. Proc Natl Acad Sci U S A. 2002;99:8295-8300.
12. Nagy KZ, Lauls S, Gentner B, et al. Clonal analysis of individual marrow repopulating cells after experimental peripheral blood progenitor cell transplantation. Stem Cells. 2004;22:570-579.
13. Borrello MA, Phipps RP. The B/macrophage cell: an elusive link between CD5+ B lymphocytes and macrophages. Immunol Today. 1996;17:471-475.
14. Hou YH, Srour EF, Ramsey H, Dahl R, Broxmeyer HE, Hromas R. Identification of a human B-cell/myeloid common progenitor by the absence of CXCR4. Blood. 2005;105:3488-3492.
15. Ito M, Hiramatsu H, Kobayashi K, et al. NOD/SCID/gamma(c)(null) mouse: an excellent recipient mouse model for engraftment of human cells. Blood. 2002;100:3175-182.
16. Yahata T, Ando K, Nakamura Y, et al. Functional human T lymphocyte development from cord blood CD34+ cells in nonobese diabetic/Shi-scid, IL-2 receptor gamma null mice. J Immunol. 2002;169:204-209.
17. Hiramatsu H, Nishikomori R, Heike T, et al. Complete reconstitution of human lymphocytes from cord blood CD34+ cells using the NOD/SCID/gammacnull mice model. Blood. 2003;102:873-880.
18. Scollay R, Smith J, Stauffer V. Dynamics of early T cells: prothymocyte migration and proliferation in the adult mouse thymus. Immunol Rev. 1986;91:129-157.
19. Bhandoola A, Sambandam A, Allman D, Meraz A, Schwarz B. Early T lineage progenitors: new insights, but old questions remain. J Immunol. 2003;171:5653-5658.
20. Glimm H, Eisterer W, Lee K, et al. Previously undetected human hematopoietic cell populations with short-term repopulating activity selectively engraft NOD/SCID-beta2 microglobulin-null mice. J Clin Invest. 2001;107:199-206.
21. Hogan CJ, Shpall EJ, Keller G. Differential long-term and multilineage engraftment potential from subfractions of human CD34+ cord blood cells transplanted into NOD/SCID mice. Proc Natl Acad Sci U S A. 2002;99:413-418.
22. Mazurier F, Doedens M, Gan OI, Dick JE. Rapid myeloerythroid repopulation after intrafemoral transplantation of NOD/SCID mice reveals a new class of human stem cells. Nat Med. 2003;9:959-963.
23. Schmidt M, Hoffmann G, Wissler M, et al. Detection and direct genomic sequencing of multiple rare unknown flanking DNA in highly complex samples. Hum Gene Ther. 2001;12:743-749.
24. Ando K, Yahata T, Sato T, et al. Direct evidence for ex vivo expansion of human hematopoietic stem cells. Blood. 2006;107:3371-3377.
25. Dean FB, Hosono S, Fang L, et al. Comprehensive human genome amplification using multiple displacement amplification. Proc Natl Acad Sci U S A. 2002;99:5261-5266.
26. Hosono S, Faruqi AF, Dean FB, et al. Unbiased whole-genome amplification directly from clinical samples. Genome Res. 2003;13:954-964.
27. Mazurier F, Gan OI, McKenzie JL, Doedens M, Dick JE. Lentivector-mediated clonal tracking reveals intrinsic heterogeneity in the human hematopoietic stem cell compartment and culture-induced stem cell impairment. Blood. 2004;103:545-552.
28. Nash R, Storb R, Neiman P. Polyclonal reconstitution of human marrow after allogeneic bone marrow transplantation. Blood. 1988;72:2031-2037.
29. Turhan AG, Humphries RK, Phillips GL, Eaves AC, Eaves CJ. Clonal hematopoiesis demonstrated by X-linked DNA polymorphisms after allogeneic bone marrow transplantation. N Engl J Med. 1989;320:1655-1661.
30. Brenner MK, Rill DR, Moen RC, et al. Gene-marking to trace origin of relapse after autologous bone-marrow transplantation. Lancet. 1993;341:85-86.
31. Dunbar CE, Cottler-Fox M, O'Shaughnessy JA, et al. Retrovirally marked CD34-enriched peripheral blood and bone marrow cells contribute to long-term engraftment after autologous transplantation. Blood. 1995;85:3048-3057.
32. Kohn DB, Weinberg KI, Nolta JA, et al. Engraftment of gene-modified umbilical cord blood cells in neonates with adenosine deaminase deficiency. Nat Med. 1995;1:1017-1023.
33. Schmidt M, Carbonaro DA, Speckmann C, et al. Clonality analysis after retroviral-mediated gene transfer to CD34+ cells from the cord blood of ADA-deficient SCID neonates. Nat Med. 2003;9:463-468.
34. Schmidt M, Hacein-Bey Abina S, Wissler M, et al. Clonal evidence for the transduction of CD34+ cells with lymphomyeloid differentiation potential and self-renewal capacity in the SCID-X1 gene therapy trial. Blood. 2005;105:2699-2706.
35. Leonard WJ, Shores EW, Love PE. Role of the common cytokine receptor gamma chain in cytokine signaling and lymphoid development. Immunol Rev. 1995;148:97-114.
36. Miller JS, McCullar V, Punzel M, Lemischka IR, Moore KA. Single adult human CD34(+)Lin-CD38(-) progenitors give rise to natural killer cells, B-lineage cells, dendritic cells, and myeloid cells. Blood. 1999;93:96-106.
37. Robin C, Pflumio F, Vainchenker W, Coulombel L. Identification of lymphomyeloid primitive progenitor cells in fresh human cord blood and in the marrow of nonobese diabetic severe combined immunodeficient (NOD/SCID) mice transplanted with human CD34(+) cord blood cells. J Exp Med. 1999;189:1601-1610.

38 Goldschneider I, Komschlies KL, Greiner DL. Studies of thymocytopoiesis in rats and mice, I: kinetics of appearance of thymocytes using a direct intrathymic adoptive transfer assay for thymocyte precursors. J Exp Med. 1986;163:1-17.

39 Allman D, Sambandam A, Kim S, et al. Thymopoiesis independent of common lymphoid progenitors. Nat Immunol. 2003;4:168-174.

40 Dick JE. Stem cells: self-renewal writ in blood. Nature. 2003;423:231-233.

41 Osawa M, Nakamura K, Nishi N, et al. In vivo self-renewal of c-Kit + Sca-1 + Lin(low/) hemopoietic stem cells. J Immunol. 1996;156:3207-3214.

42 Pawliuk R, Eaves C, Humphries RK. Evidence of both ontogeny and transplant dose-regulated expansion of hematopoietic stem cells in vivo. Blood. 1996;88:2852-2858.

43 Holyoake TL, Nicolini FE, Eaves CJ. Functional differences between transplantable human hematopoietic stem cells from fetal liver, cord blood, and adult marrow. Exp Hematol. 1999;27:1418-1427.

44 Cashman J, Dykstra B, Clark-Lewis I, Eaves A, Eaves C. Changes in the proliferative activity of human hematopoietic stem cells in NOD/SCID mice and enhancement of their transplantability after in vivo treatment with cell cycle inhibitors. J Exp Med. 2002;196:1141-1149.

45 Rosendaal M, Hodgson GS, Bradley TR. Organization of haemopoietic stem cells: the generation-age hypothesis. Cell Tissue Kinet. 1979;12:17-29.

46 Harrison DE, Astle CM. Loss of stem cell repopulating ability upon transplantation. Effects of donor age, cell number, and transplantation procedure. J Exp Med. 1982;156:1767-179.

47 Allsopp RC, Morin GB, Horner JW, DePinho R, Harley CB, Weissman IL. Effect of TERT overexpression on the long-term transplantation capacity of hematopoietic stem cells. Nat Med. 2003;9:369-371.

48 Ema H, Sudo K, Seita J, et al. Quantification of self-renewal capacity in single hematopoietic stem cells from normal and Ink-deficient mice. Dev Cell. 2005;8:907-914.

49 Bonnet D, Dick JE. Human acute myeloid leukemia is organized as a hierarchy that originates from a primitive hematopoietic cell. Nat Med. 1997;3:730-737.

50 Hope KJ, Jin L, Dick JE. Acute myeloid leukemia originates from a hierarchy of leukemic stem cell classes that differ in self-renewal capacity. Nat Immunol. 2004;5:738-743.